Greenhouse gasses emissions and their trends over the last three decades across Africa

Mounia Mostefaoui[1], Philippe Ciais[2], Matthew J. McGrath[2], Philippe Peylin[2], Prabir K. Patra[3], Yolandi Ernst[4]

[1]Laboratoire de Météorologie Dynamique/IPSL, École Normale Supérieure, PSL Research University, Sorbonne University, École Polytechnique, IP Paris, CNRS, Paris, France.
[2]Laboratoire des Sciences du Climat et de l'Environnement, 91190 Gif-sur-Yvette, France.
[3]Research Institute for Global Change, JAMSTEC, Yokohama 2360001, Japan.
[4]Global Change Institute, University of the Witwatersrand, Johannesburg, South Africa.

Correspondence to: mounia.mostefaoui@polytechnique.edu

Key words: greenhouse gasses, anthropogenic emissions and removals, fossil fuels, land-use, land-use change and forestry, Africa, bottom-up, top-down atmospheric inversions, UNFCCC inventories, Global Carbon Project, PRIMAP-hist, IPCC sectors, climate change, Paris Agreement, Global Stocktake, Monitoring, Reporting and Verification.

Abstract. A key goal of the Paris Agreement (PA) is to reach net-zero Greenhouse Gasses (GHG) emissions by 2050 globally, which requires mitigation efforts from all countries. Africa's rapidly growing population and GDP makes this continent important for GHG emission trends. In this paper, we study the emissions of carbon dioxide (CO_2), methane (CH_4) and nitrous oxide (N_2O) in Africa over three decades (1990-2018). We compare bottom-up (BU) approaches including UNFCCC national inventories, FAO, PRIMAP-hist, process-based ecosystem models for CO_2 fluxes in the Land Use, Land Use Change and Forestry (LULUCF) sector, and global atmospheric inversions. For inversions, we applied different methods to separate anthropogenic CH_4 emissions. The BU inventories show that over the decade 2010-2018, less than ten countries represented more than 75% of African fossil CO_2 emissions. With a mean of 1373 $MtCO_2$ yr^{-1}, total African fossil CO_2 emissions over 2010-2018 represent only 4% of global fossil emissions. Yet, these emissions grew by +34% from 1990-1999 to 2000-2009 and by +31% over 2000-2009 to 2010-2018, which represent more than a doubling in 30 years. This growth rate is more than twice faster than the global growth rate of fossil CO_2 emissions. The anthropogenic emissions of CH_4 grew by 5% from 1990-1999 to 2000-2009 and by 14.8% from 2000-2009 to 2010-2018. The N_2O emissions grew by 19.5% from 1990-1999 to 2000-2009; and by 20.8% from 2000-2009 to 2010-2018. When using the mean of estimates from UNFCCC reports (including the land use sector), with corrections from outliers, Africa was a mean source of greenhouse gasses of 2622^{3239}_{2186} $MtCO_2e$ yr^{-1} from all BU estimates (sub- and superscript indicating min-max range uncertainties), and of $+2637^{5873}_{1761}$ $MtCO_2e$ yr^{-1} from top-down (TD) methods, during their overlap period from 2001 to 2017. Although the mean values are consistent, the range of) TD estimates is larger than the one of BU estimates, indicating that sparse atmospheric observations and transport model errors do not allow us to use inversions to reduce the uncertainty of BU estimates. A main source of uncertainty comes from CO_2 fluxes in the land-use sector (LULUCF) for which the spread across inversions is larger than 50%, especially in Central Africa. Moreover, estimates from national UNFCCC communications differ widely depending on whether the large sinks in a few countries are corrected to more plausible

values using more recent national sources following the methodology of Grassi et al. (2022). The median of CH_4 emissions from inversions based on satellite retrievals and surface station networks are consistent with each other within 2% at continental scale. The inversion ensemble also provides consistent estimates of anthropogenic CH_4 emissions with BU inventories such as PRIMAP-hist. For N_2O, inversions systematically show higher emissions than inventories, on average about 4.5 times more than PRIMAP-hist, either because natural N_2O sources cannot be separated accurately from anthropogenic ones in inversions, or because BU estimates ignore indirect emissions and under-estimate emission factors. Future improvements can be expected thanks to a denser network for monitoring atmospheric concentrations. This study helps to introduce methods to enhance the scope of use of various published datasets and allows to compute budgets thanks to recombinations of those data products. Our results allow to understand uncertainty and trends of emissions and removals in a region of the world where few observations exist and most inventories are based on default IPCC guidelines values. The results can therefore serve as a support tool for the Global Stocktake (GST) of the Paris Agreement. The referenced datasets related to figures are available at: https://doi.org/10.5281/zenodo.7347077 (Mostefaoui et al., 2022).

Introduction

Large global reductions of greenhouse gasses (GHG) emissions are needed to avoid "dangerous anthropogenic interference with the climate system" (IPCC, 2021). The Paris Agreement (PA) aims at limiting global warming below 2°C and reaching "net-zero GHG emissions by 2050" (UNFCCC, 2015). To improve the monitoring of emissions trends, the PA has an Enhanced Transparency Framework (ETF) by which countries will have to report their GHG emissions and removals under a standardized format starting in 2024 (Perugini et al., 2021; UNFCCC, 2021) through Biennial Transparency Reports (BTR), with the ambition to use up-to-date data and best available science to improve national inventories. This represents a challenge for many developing countries, where emissions inventories have been irregular.

Recent analyses predict a fast increase of African emissions correlated with demographic growth. The African population is expected to double from 1.2 billion in 2019 to 2.5 billion at the 2050 horizon (UN, 2019). Using the TIAM-ECN Integrated Assessment Model (IAM) developed with data from the International Energy Agency (IEA), van der Zwaan et al., (2018) concluded that greenhouse gasses (GHG) emissions from Africa will become substantial at the global scale by 2050. In Shared Socio-economic Pathways (SSP) projection scenarios, Africa and the Middle East are grouped together despite having very different geographies, per capita emissions and Gross Domestic Product (GDP) (IIASA, 2017). According to IAM projections, the minimum projected share of Africa in global emissions would be close to 10% by 2050 for a business-as-usual pathway. An "explosive growth in African combustion emissions" (Liousse et al., 2014) could not be excluded from 2030 to 2050, if no drastic mitigation policies are implemented (IPCC, 2021). If a stringent emissions reduction pathway limiting global warming to +2 °C is adopted, Africa could contribute to around 20% of global emissions by 2050, becoming the second largest worldwide emitting region. Further, under stringent climate policy scenarios, CH_4 and N_2O emissions in Africa were projected to contribute 80% of the total emissions of these two gasses in 2050 (van der Zwaan et al., 2018). Therefore, Africa will become an important global emission contributor under any mitigation pathway with a demographical and industrial development increase.

There are 56 African countries represented in the United Nations. National emissions reports to the United Nations Convention Framework on Climate Change (UNFCCC) are available for 53 countries, including all major African emitters. Africa as a whole ranks fifth worldwide in terms of territorial fossil fuels use with a total of 1449 $MtCO_2e$, in-between the Russian Federation and Japan (Friedlingstein et al., 2020). The global share of Africa is ~ 4% of fossil CO_2 (FCO_2) emissions, ~ 16

84 % of CH_4 emissions (Saunois et al., 2020) and ~ 25% of N_2O emissions (Tian, 2020). South Africa is

85 the biggest FCO_2 emitter in the continent, and ranked twelve on the global scale, just after Brazil.

86 Despite projections of strong growth of emissions and population in Africa, the continent is under-

87 studied and lacks up-to-date comprehensive assessments of GHG emissions and removals, given

88 sporadic and often outdated reports by individual countries. The literature tends to be scarce about

89 African countries, and their emissions have rarely been analyzed comprehensively using the results

90 from both statistical inventories that are also referred to as bottom-up (BU) methods, and from top-

91 down (TD) atmospheric inversions. Country reports estimate GHG emissions through statistical

92 inventories using estimates of national sectoral activity data multiplied by emissions factors, with three

93 levels of refinements depending on countries, named Tier 1 for default emissions factors, Tier 2 for

94 country-specific emissions factors / activity data and Tier 3 for more emissions factors / activity with

95 tailored representation at the scale of process. Other BU inventories for assessing national emissions

96 also exist: they are based on the same approach as country-reported inventories but use their own

97 parameters for activity data and emissions factors coming from research groups, international statistical

98 agencies, etc. Process-based ecosystem models developed by the research community are not used by

99 countries. They are based on the representations of complex ecosystem processes and can also be

100 viewed as a BU method. Besides, another approach is named "top-down" and refers to atmospheric

101 inversions. Inversions consist in estimating causes (emissions and sinks) based on consequences

102 (concentrations). The inverse modeling approach consists in adjusting a priori fluxes to the atmospheric

103 transport in order to be as adjusted as possible with observation data by minimizing a cost function.

104 This is a mathematically complex problem under constrained because every point of the globe is an

105 unknown emission, and there is only a limited number of observations: "regularization" techniques are

106 used to find a unique solution. The African ground-based atmospheric network used by inversions is

107 very sparse. There are only three currently active surface flasks over this whole continent, located in

108 Namibia (Gobabeb), in the Seychelles (Mahe Island), and in South Africa (Cape Point). The one in

109 Algeria (Assekrem) was terminated on 26/08/2020, and the one in Kenya has been inactive since

110 21/06/2011. The characteristics of the surface flasks in Africa, available on the NOAA website are

111 summarized in Table S1. Inversion results are therefore uncertain due to this small number of

112 atmospheric stations over the continent (Nickless et al., 2020).

113 A previous analysis of African emissions was solely focused on FCO_2 emissions during the decade

114 2000-2009 (Canadell et al., 2009). A first budget for the period 1990-2009 was provided at the

115 continental scale with the RECCAP1 project (Valentini et al., 2014). Ayompe et al. (2020) studied

116 recent FCO_2 emissions trends, using International Energy Agency (IEA) data. Other studies are region-

specific or sector-specific, focusing exclusively on agriculture (Bombelli et al., 2009), on natural ecosystems in Sub-Saharan Africa (Kim et al., 2016) or in individual countries such as Kenya (Zhu et al., 2018).

Paying attention not only to commonly identified big emitters like South Africa, but also to medium emitters and to emerging emitters is important, not only in terms of scientific assessment, but also for financial and climate policy purposes under the PA. The Monitoring, Reporting and Verification (MRV) provisions of the PA indeed require scientific and policy tools to verify the pledges made by all the signatory countries. Instruments for financial transfers for mitigation and adaptation like the Green Fund on Climate Change (GCF) and the REDD+ initiatives cover the African scope and will require scientific assessment of trends for impact evaluation and credibility purposes, and as an incentive for continued investments. As part of the Global Stock Take (GST) under article 14 of the PA aiming at assessing "collective progress", all signatory parties will have to show their contributions to the global mitigation efforts. These efforts will be evaluated within a MRV system which includes the requirement for developing countries to submit their Biennial Update Reports (BUR) on a biennial basis starting in 2024. As no standard global reporting framework has been required to date, we anticipate that the data available for the first stocktake in 2023 will be very heterogeneous. As a continent gathering non-Annex I countries exclusively, the African case is featured by the scarcity of national official inventories which have been provided to date on a voluntary basis through National Communication (NC) and BUR. BU estimates of emissions established by independent scientific methods are also discussed in the present study. In this context, different and complementary observation-based methods assessing national GHG emissions and sinks are needed.

The aim of this paper is to evaluate relative merits of different existing types of datasets for the assessment of African emissions and removals and their trends for CO_2, CH_4 and N_2O during the last three decades. In this paper, we standardize the metrics and scope of application for different categories of GHG emissions to discuss budgets. We also validate and benchmark different independent datasets to evaluate the possibility to use them as a verifying tool for official country-reported data. In order to cover all GHG sectors, we also describe recombinations of different historical datasets for the last 30 years that are necessary to fill the gap for some missing past sectoral emissions. This study offers a comparison of data products originally combined to compute a budget and an evaluation of their relative merits. The different data products discussed here include different BUapproaches, including official countries communications to the UNFCCC and estimations from the Food and Agriculture Organization (FAO), Carbon Dioxide Information Analysis Center (CDIAC), global inventories for anthropogenic emissions (PRIMAP-hist which integrates combinations of various datasets including

FAO and Global Carbon Project (GCP)), and process-based models for land CO_2 fluxes with 14 Dynamic General Vegetation Models (DGVM) from the TRENDY version 9 ensemble (Table 1). We also analyze and combine TD products to discuss individual gas and to compute budgets: three atmospheric global inversions for CO_2 land fluxes; 22 inversions for CH_4 emissions (11 inversion models using surface station data and 11 satellite inversion models) and CH_4 wildfire emissions from the Global Fires Emission Dataset (GFED) version 4. We used three inversion models for N_2O fluxes (PyVAR model, TOMCAT-INVICAT model, and MIROC4-ACTM model (see Table 1). Inversions only solve for total fluxes or at best for groups of sectors, whereas BU estimates have a larger number of sectors. In Table 2, we present the correspondence between 'sectors' defined by the TD and BU methods. For all datasets, we chose an atmospheric convention with negative values representing removals from the atmosphere (i.e. land sink). We deliver an original comparison of BU estimates from national inventories, global inventories, and process-based models, with TD estimates from atmospheric inversions over Africa. The work is carried out for large countries or groups of small countries, as inversions do not have the capability to constrain fluxes over small areas given their coarse grid and sparse atmospheric data. Based on the benchmarking and relative merits evaluation of the various data products presented above, the scientific questions addressed in this study are: 1) How consistent are the mean values and trends of GHG emissions across BU estimates in Africa? 2) How consistent are the different inversion model results? 3) How do inversions compare with BU estimates? 4) What is the net GHG balance of the African continent from different observation-based methods, including CO_2 sinks and sources in the land-use sector? 5) What are the main sources of uncertainties? The manuscript is organized into two main sections. First, a material and methods section describes the regional breakdown and input data (section 1). We present our results for the whole Africa and for six groups of aggregated countries (section 2) with a specific analysis of CO_2 emissions and sinks, divided between FCO_2 (section 2.1), fluxes in the land use, land use change and forestry (LULUCF) sector (section 2.2), and emissions of non-CO_2 greenhouse gasses (sections 2.3 and 2.4). Conclusions are drawn about uncertainties of African GHG net emissions and removals assessment.

1 Methods, datasets and datasets usage

This study covers the period from 1990 to 2018, and emissions and sinks of CO_2, CH_4 and N_2O. We used 1990 as a base year since reporting to the UNFCCC mostly started in that year and is often used as a reference comparison year in national pledges of the PA. The last year of analysis is 2018, reflecting the availability of inversion data and avoiding further uncertainty due to poorly understood

183 emissions changes before and after the COVID19 crisis. This period allows the analysis of decadal
184 features. It also has the advantage of being covered by several datasets, listed in Table 1. We considered
185 different BU approaches, including official countries communications to the UNFCCC and estimations
186 from the Food and Agriculture Organization (FAO), global inventories for anthropogenic emissions
187 (PRIMAP-hist which integrates combinations of various datasets including FAO, GCP, EDGAR
188 v4.3.2, Andrew 2018 cement data, BUR, Common Reporting Format (CRF), UNFCCC data, and BP),
189 and process-based models for land CO_2 fluxes with 14 Dynamic General Vegetation Models (DGVM)
190 from the TRENDY version 9 ensemble (Table 1). We used three atmospheric global inversions for CO_2
191 land fluxes; 22 inversions for CH_4 emissions; and three inversions for N_2O fluxes (Table 1). For
192 preliminary data quality control, we checked the consistency of prior fluxes by plotting them separately
193 (Fig. S1). Inversions only solve for total fluxes or at best for groups of sectors, whereas BU estimates
194 have a larger number of sectors. In Table 2, we present the correspondence between 'sectors' defined
195 by the TD and BU methods. For all datasets, we chose an atmospheric convention with negative values
196 representing removals from the atmosphere (i.e. land sink). No specific standard guidelines currently
197 exist for defining uncertainties of BU and TD data products. Given that some of our estimates are based
198 on a small number of models / estimates, we cannot calculate the full distribution e.g. with a 95%
199 confidence interval, but we rather reported ranges with min / max. Assuming that the unknown
200 distributions would be Gaussian, like in Schulze et al. (2018), we could infer a 2-sigma ($\approx$ 95%)
201 confidence interval if we assume that min-max are equivalent to 3-sigma, but in view of the small
202 numbers of estimates e.g. for N_2O with only 3 inversions, we prefer to just give the min-max range.
203 Moreover, for national inventories, as all African countries are non-Annex I, they do not deliver
204 confidence intervals but Grassi et al. (2022) estimated for CO_2 LULUCF fluxes uncertainties of 50 %
205 for the average of non-Annex-1 countries. Here uncertainty estimates are understood as the spread
206 among minimum and maximum values from one methodology. A main source of uncertainty in the
207 comparison of country-reported data with other data products is the inclusion or not of natural fluxes
208 additionally to anthropogenic emissions sectors. For the comparability of the different data products
209 presented in this study, we discuss only the mean value over the period of overlapping data availability.
210 Referenced datasets are available at https://doi.org/10.5281/zenodo.7347077 (Mostefaoui et al., 2022).

211

212

213

214

Table 1. List of BU and TD methods used. (For more details, see also Saunois et al. (2020) for CH_4, Friedlingstein et al. (2020) for FCO_2; UNFCCC country-reported data; Gütschow et al. (2021) for PRIMAP-hist).

Dataset name	Method	CO_2	CH_4	N_2O	Spatial resolution	Time period covered
Inversions						
Global Carbon Budget ensemble (2020) [1]	TD	×			from $1° \times 1°$ to $6° \times 4°$	2000-2019
Global Methane Budget ensemble [2] (2020)	TD		×		from $1° \times 1°$ to $6° \times 4°$	2000-2017 [3]
Global N_2O Budget ensemble [4] (2020)	TD			×	from $2.8° \times 2.8°$ to $5.6° \times 5.6°$	1998-2017
DGVMs						
TRENDYv9 [5]	BU				$0.5° \times 0.5°$ (land surface) or $1° \times 1°$	1990-2019
Other BU inventories						
PRIMAP-hist (excluding LULUCF)	BU	×	×	×	country	1990-2019
GCB (CDIAC) (excluding LULUCF)	BU	×			$0.1° \times 0.1°$	1990-2019
UNFCCC	BU	×			country	1990-2015
FAO (LULUCF CO_2)	BU	×			country	1990-2019
GFEDv4 (wildfires only)	BU		×		$0.25° \times 0.25°$	1997–2016

(1) See 3 inversions details in the supplementary Table S6.
(2) See 22 inversions details in the supplementary Table S7.
(3) Variations from 2003-2015, 2000-2015, 2010-2017: see detailed period coverage for each dataset in the supplementary Table S7.
(4) See 3 inversion details in the supplementary Table S8.
(5) See supplementary Table S5 for the 14 products.

Table 2. Sectoral reconciliation between categories defined in TD and BU methods.

Gas	Sector label choice for BU and TD	TD inversions	BU inventories
CO_2	Net land flux	Total Net Biome Productivity (NBP) after subtraction of prior prescribed Fossil CO_2	Energy + Industrial Processes and Product Use + Agriculture + Waste + Biomass burning
CH_4	Total anthropogenic emissions	Fossil + Anthropogenic Biomass burning + Agriculture & Waste - Wildfires	Energy + Industrial Processes + Agriculture + Waste + Biomass burning
N_2O	Total	Total	All IPCC sectors

1.1 Regional breakdown

As some countries are small emitters and their area is too small to be resolved by inversions, and in some cases even by DGVMs, we grouped African countries into six regions shown in Fig. S2 and listed in Table S2. The grouping followed national borders and biomes similarity considering the Köppen-Geiger climate zones (Beck et al., 2018), magnitudes of fossil fuel emissions, and per capita emissions (Fig. S2, Fig. S3 and Fig. S8). We also grouped a maximum of about ten countries per region.

1.2 Inventories datasets

PRIMAP-hist anthropogenic emissions assessment for CO_2, CH_4, and N_2O

The PRIMAP-hist version 2.2 BU dataset is derived from Gütschow et al., (2021) and combines UNFCCC reports with a gap-filling method to produce a time series of annual anthropogenic emissions for different IPCC sectors. PRIMAP-hist does not cover the LULUCF sector for CO_2 due to the high uncertainties. PRIMAP-hist does not include emissions from shipping and international aviation, but includes cement as part of FCO_2 emissions. We use data from the HISTCR scenario (data accessed from https://www.pik-potsdam.de/paris-reality-check/primap-hist/ in April 2022) from country-prioritized dataset, which mainly uses UNFCCC (BUR and NC) data, unless such data are missing, in that case PRIMAP-hist uses extrapolated data from EDGAR (2021), FAO (2021) and BP Statistical Review of World Energy (2021).

Global Carbon Project (GCP) fossil CO₂ emissions

We used country-level FCO$_2$ data published by the global CO$_2$ budget by the Global Carbon Project (GCP) (Friedlingstein et al., 2020) separated per fuel type (gas, oil and coal) and including fossil fuel use in the combined industry, ground transportation and power sectors, natural gas flaring, cement production, and process-related emissions (e.g. fertilizers and chemicals). Data for African countries coming among others from the Carbon Dioxide Information Analysis Center (CDIAC) compiled until 2018 (Gilfillan & Marland, 2021), BP Statistical Review of World Energy (BP, 2020), and recent estimates of cement production and clinker-to-cement ratios (Andrew, 2020).

UNFCCC inventories for CO₂ in the LULUCF sector

We used UNFCCC submissions for LULUCF CO$_2$ fluxes from NC and BUR reports downloaded from the UNFCCC website (https://unfccc.int/) in March 2021, and further processed into .csv tables by Deng et al., (2021). Those estimates are based on different accounting methods following the IPCC Guidelines (IPCC, 2006; IPCC, 2019). Country-reported data quality control, quality assurance and verification process follow 2006 IPCC guidelines detailed in Chapter 6 QA/QC procedures of this document. African countries, being Non-Annex I countries, do not report emissions every year. Figure 1 shows the number of BUR and NC provided each year per African region. The years 1990, 1994, 1995, 2000 and 2005 are featured with several updates, while most of the other years have few updates. About every two years, all regions have at least one update. Note that flexibility for BUR is given to Least Developed Countries (LDCs), that include 33 out of 56 African countries, and to Small Islands Developing States (SIDS), that include six African countries (Table S4).
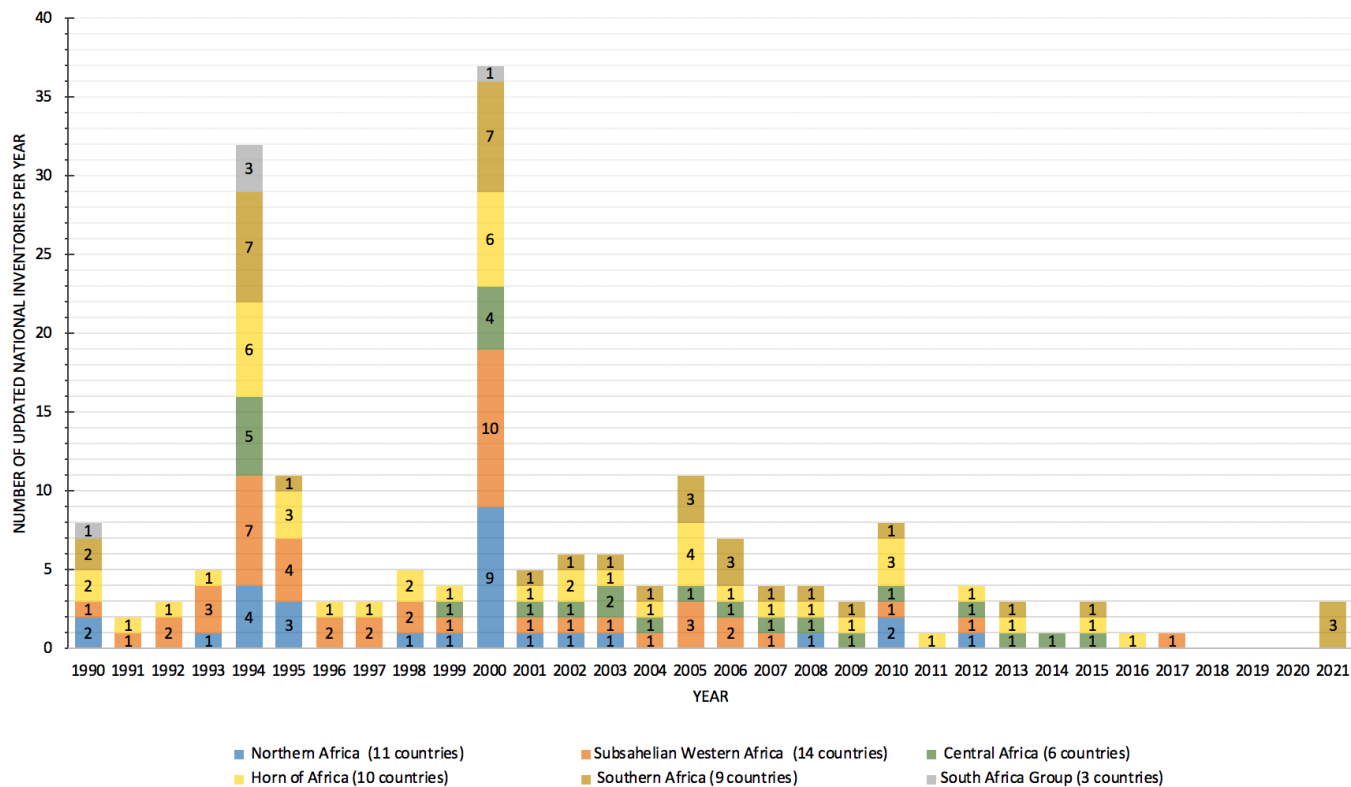
Figure 1. Number of UNFCCC reports for LULUCF CO$_2$ fluxes in National Communications and Biennial Update Reports, per group of countries defined in Table S2.

Non-Annex I African countries can use older versions of the IPCC guidelines (IPCC, 2006; IPCC, 2019a). This induces uncertainties from changes in accounting methods between versions, with recent guidelines having more detailed sectors and sources. There is no data for Libya, Equatorial Guinea, Malawi and Sierra Leone during the whole period. UNFCCC data are missing in some years for Rwanda, Sao Tome & Principe, Senegal, South Sudan, Angola. There is no data during 1990-1998 for Liberia.

We noticed that NC and BUR lack details regarding the methods used, the sources for activity data and emissions factors, and most of them are in French language. BUR in .pdf format include a non-standardized table for emissions. The reader is sometimes referred to the "national coordinator for climate change service" with no link to any database or contact person.

Because the PA targets human-induced emissions, countries use the proxy of "Managed lands" for the LULUCF sector, as defined by the IPCC guidelines (https://www.ipcc-nggip.iges.or.jp/public/2006gl/vol4.html; last accessed in August 2022). Managed lands are areas where LULUCF CO$_2$ fluxes are assigned to some anthropogenic activities. Several African NC and BUR do not contain information on their managed lands areas. We thus looked at REDD+ national reports (https://redd.unfccc.int/submissions.html?topic=6; last accessed in August 2022) to get this information

279 (Fig. S3 and Table S9). LULUCF CO_2 fluxes on managed lands result from either direct anthropogenic
280 effect such as land use change and forestry, or indirect effects (such as change in CO_2 and climate) on land
281 remaining in the same land use, e.g. forest remaining forest (Grassi et al., 2022). The vast majority of African
282 countries use a Tier 1 IPCC accounting method which does not distinguish between these different effects.
283 Tier 1 methods use a classification with only three out of six possible types of land: "forest land", "cropland"
284 and "grassland", and do not give spatially explicit land use data. Tier 2 methods include fluxes from six
285 land use types: forest, cropland and grassland, wetlands, urban and other land-use, for the case of land
286 remaining under the same land use type, and for the case of conversions between land use types. In Africa,
287 only South Africa and Zambia used Tier 2 methods for some LULUCF CO_2 subsectors.
288
289 **Processing of the UNFCCC LULUCF CO_2 data and outliers correction**
290 We processed the UNFCCC LULUCF CO_2 data for outlier corrections (Table S5). For Guinea-Bissau, and
291 Tanzania, we identified inconsistent values from successive communications with substantially differing
292 numbers. For Guinea, Madagascar, Zimbabwe, Congo, Mali, the Central African Republic (CAF), Angola
293 and Mauritius we identified changes of more than one order of magnitude between two consecutive reports
294 and likely implausibly large carbon sinks considering their national forest area. The computations of per
295 area emissions and removals showed discrepancies, which points out the need for further examination and
296 inspection of more recent reports in NDC and REDD+ reports (Table S5). Our corrections explained in the
297 supplementary section are consistent with those proposed by Grassi et al. (2022) who diagnosed
298 'biophysically impossible' sequestration rates with a threshold value larger than 10 tCO_2/ha yr^{-1} over an
299 area greater than 1 Mha. For Namibia, Nigeria and the Democratic Republic of the Congo (DRC), it was
300 challenging to select a best estimate between recent and past reports. For those countries, corrections using
301 more recent data than BUR/NC have high uncertainties, as noted by Grassi et al. (2022). This includes the
302 absence of any sink for DRC for instance, contrary to sinks consistently reported over time and large forested
303 area in this country's previous reports to the UNFCCC. We therefore systematically looked at corrected
304 values for both case scenarios (with and without Namibia, Nigeria and DRC data corrections). In total, we
305 corrected 13 outliers as shown in Table S5, consistently with Grassi et al. (2022).
306
307 **Food and Agriculture Organization of the United Nations (FAO) LULUCF CO_2 fluxes**
308 We used data from LULUCF CO_2 fluxes over 1990-2019 from the FAO Global Forests Resource
309 Assessments (FAO FRA; data License: CC BY-NC-SA 3.0 IGO, extracted from: https://fra-data.fao.org;
310 date of Access: May 2022). According to the 2005 FAO categories and definitions, forest is land covering
311 at least 0.5 hectares and having vegetation taller than 5 meters with a canopy cover higher than 10%. Other

wooded lands refer to land that are not classified as "forest" but that are wider than 0.5 ha, have a canopy cover of 5%-10% or combine trees, shrubs and bushes with cover higher than 10%. The FAO data for forests comprise carbon stock changes from both aboveground and belowground living biomass pools. They are independent from country-reported UNFCCC emissions and removals. The FAO estimates are based on activity data, areas of forest land and CO_2 emissions and removals factors. The FAO data reports: 1) net emissions and removals from "forest land remaining forest land" and from "land converted to forest" grouped together, and 2) emissions from "net forest conversion", i.e. deforestation. In contrast, the UNFCCC accounting uses a 20-years window for CO_2 fluxes from land use change, while land-use change fluxes from land-converted-to-forest are reported separately from those of 'forest remaining forest'.

1.3 Dynamic Global Vegetation Models (DGVM) datasets

We used Net Biome Productivity (NBP) from 14 Dynamic Global Vegetation Models (DGVM) from the TRENDY v9 ensemble covering the period 1990-2019. The different models described in Friedlingstein et al. (2019) are: CABLE, CLASS, CLM5, DLEM, ISAM, JSBACH, JULES, LPJ, LPX, OCN, ORCHIDEE-CNP, ORCHIDEE-SDGVM, and SURFEX (Table S6). DGVM are forced by historical reconstructions of land cover change, atmospheric CO_2 concentration and climate since 1901. Detailed cropland management practices are generally ignored, except for the harvest of crop biomass. Forest harvest is prescribed from historical statistics in 11 models (Table A1, of Friedlingstein et al., (2020)). The models simulate carbon stock changes in biomass, litter and soil pools. From the difference between simulations with and without historical land cover change, a flux called 'land use emissions' can be obtained from DGVM. This flux includes the indirect effects of climate and CO_2 on lands affected by land use change, and a foregone sink called "loss or gain of atmospheric sink capacity", which is absent from the methods used by UNFCCC and FAO. Pongratz et al. (2014) delivered the following definition of loss of sink capacity as "the CO_2 fluxes in response to environmental changes on managed land as compared to potential natural vegetation. Historically, the potential natural vegetation would have provided a foregone sink as compared to human land use." Thus, land use change fluxes from DGVM were not compared with other estimates. Note that DGVM do not explicitly separate managed and unmanaged land. Thus, we used all forest lands to calculate their mean CO_2 fluxes.

1.4 Atmospheric inversions datasets

CO_2 inversions

344 We used the net land CO_2 fluxes excluding fossil fuel emissions (hereafter, net ecosystem exchange) from

345 three global inversions of the Global Carbon Project that cover a long period (see Table A4 of Friedlingstein

346 et al., 2020), including : CarbonTrackerEurope (CTRACKER-EU-v2019; van der Laan-Luijkx et al., 2017),

347 the Copernicus Atmosphere Monitoring Service (CAMSV18-2-2019; Chevallier et al., 2005), and one

348 variant of Jena CarboScope (JENA, sEXTocNEET_v2020; Rödenbeck et al., 2005). The GCP inversion

349 protocol recommends to use as a fixed prior the same gridded dataset of FCO_2 emissions (GCP-GridFED).

350 However, some modelers used different interpolations of this dataset, and one group used a different gridded

351 dataset (Ciais et al., 2021). We applied a correction to the estimated total CO_2 flux by subtracting a common

352 FCO_2 flux from each inversion (Figure S1 and Methodological Supplementary 1). The resulting land

353 atmosphere CO_2 fluxes, or net ecosystem exchange, cannot be directly compared with inventories aiming

354 to assess C stock changes, given the existence of land-atmosphere CO_2 fluxes caused by lateral processes.

355 This issue was discussed by Ciais et al. (2021) and a practical correction of inversions was proposed by

356 Deng et al. (2022) based on new datasets for CO_2 fluxes induced by lateral processes involving river

357 transport, crop and wood product trade. We applied here the same correction to all CO_2 inversions.

CH_4 inversions

359 We used the CH_4 emissions from global inversions over 2000-2017 from the Global Methane Budget

360 (Saunois et al., 2020) (Table 1). This ensemble includes 11 models using GOSAT satellite CH_4 total-column

361 observations covering 2010-2017, and 11 models assimilating surface stations data (SURF) since 2000

362 (Table S5). Surface inversions are constrained by very few stations for Africa, while the GOSAT satellite

363 data has a better coverage. One could thus expect GOSAT inversions to give more robust results. Inversions

364 deliver an estimate of surface net CH_4 emissions, although some of them solve for fluxes in groups of

365 sectors, called 'super-sectors'. We have not used in situ for dataset validation per se, only the GOSAT data

366 were evaluated against Total Carbon Column Observing Network (TCCON) independent ground based total

367 column-averaged abundance of CH_4 (XCH4). In the inversion dataset, net CH_4 surface emissions were

368 interpolated into a $0.8° \times 0.8°$ resolution, regridded from coarser resolution fluxes and separated into 'super-

369 sectors' either using prior emission maps or posterior estimates for those inversions solving fluxes per

370 supersector, following Saunois et al. (2020). More specifically, these five super-sectors are: 1) Fossil Fuel,

371 2) Agriculture and Waste, 3) Wetlands, 4) Biomass and Biofuel Burning (BBUR), and 5) Other natural

372 emissions. We separated CH_4 anthropogenic emissions from inversions using Method 1 and Method 2

373 proposed by Deng et al. (2021). Method 1 relies on the separation calculated by each inversion except for

374 the BBUR supersector from which wildfire emissions were subtracted based on the Global Fires Emission

375 Dataset (GFED) version 4 (van der Werf et al., 2017). Method 2 removes from total emissions the median

376 of natural emissions from inversions (Deng et al. 2022). The two methods gave similar results and only

377 Method 1 was used in the results section.

378

379 **N$_2$O inversions**

380 We used three N$_2$O atmospheric inversions from the global N$_2$O budget synthesis (Tian, 2020) and from

381 Deng et al. (2022) (Tables S1 and S7) : PyVAR CAMS (Thomson et al., 2014), MATCM_JMASTEC

382 (Rodgers, 2000), (Patra et al., 2018), and TOMCAT (Wilson et al., 2014; Monks et al., 2017). We used the

383 total N$_2$O flux from inversions including natural emissions, given that natural emissions estimates are highly

384 uncertain for Africa. Inversion results are therefore not directly comparable with the PRIMAP-hist inventory

385 which only contains anthropogenic emissions.

386
387 **1.5 Metrics to compare gasses and ancillary data and data usage**

388

389 We express emissions of non-CO$_2$ gasses in megatons of carbon dioxide equivalent (MtCO$_2$e) using the

390 Global Warming Potential over a 100-year time horizon (GWP100) values from the fourth IPCC

391 Assessment Reports (IPCC AR4, WGI Chapter 2, 2007), consistent with PRIMAP-hist and historical

392 country-reported data. We used AR4 GWP100 because many African countries have been following the

393 2006 IPCC guidelines referring to AR4 GWP100 2019 refinement to IPCC guidelines, which do not

394 recommend any specific metrics, therefore we are following IPCC guidelines used by countries. The

395 multiplicative coefficients to use to change AR4 to AR6 GWP100 values are: 1.19 for fossil CH$_4$, 1.09 for

396 non-fossil CH$_4$, and 0.92 for N$_2$O. We used population data from the United Nations population (World

397 Population Prospects 2019, 2022), for computing per capita FCO$_2$ emissions and their disparities, based on

398 Gini indices (Dortman et al., 1979) for measuring statistical dispersions among a given population

399 (methodological supplementary M2). We also used African GDP data (World Bank, 2017).

400

401 **2 Results and discussion**

402   **2.1 Fossil CO$_2$ emissions**

403   **2.1.1 Continental, regional and country changes**

404

405

406

407

408

409   **(a)**
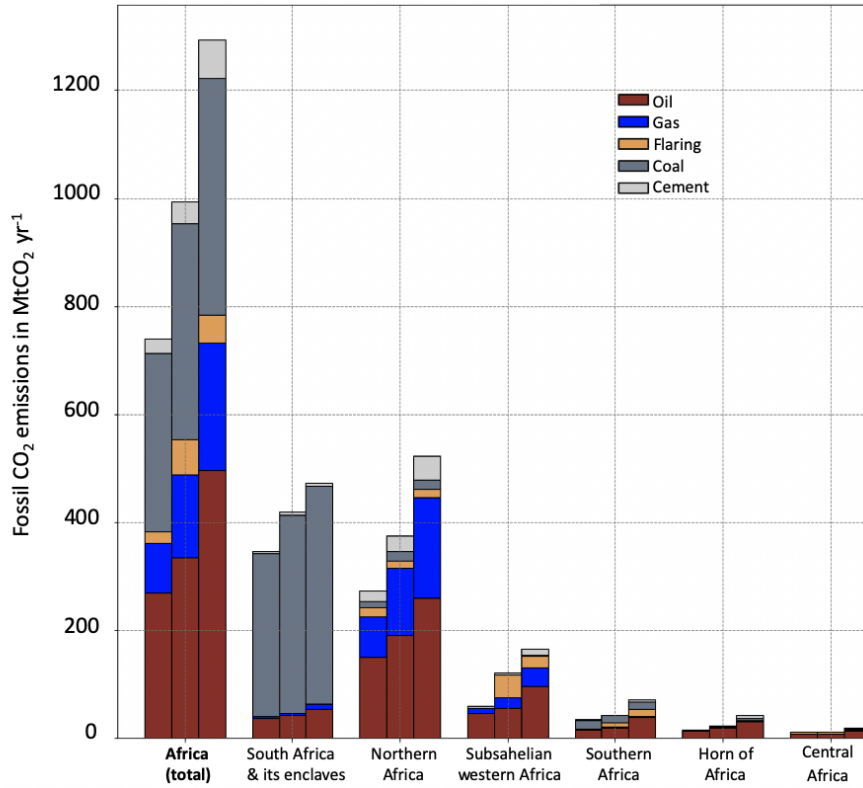
410
411   **(b)**

412
413
414
415

(c)
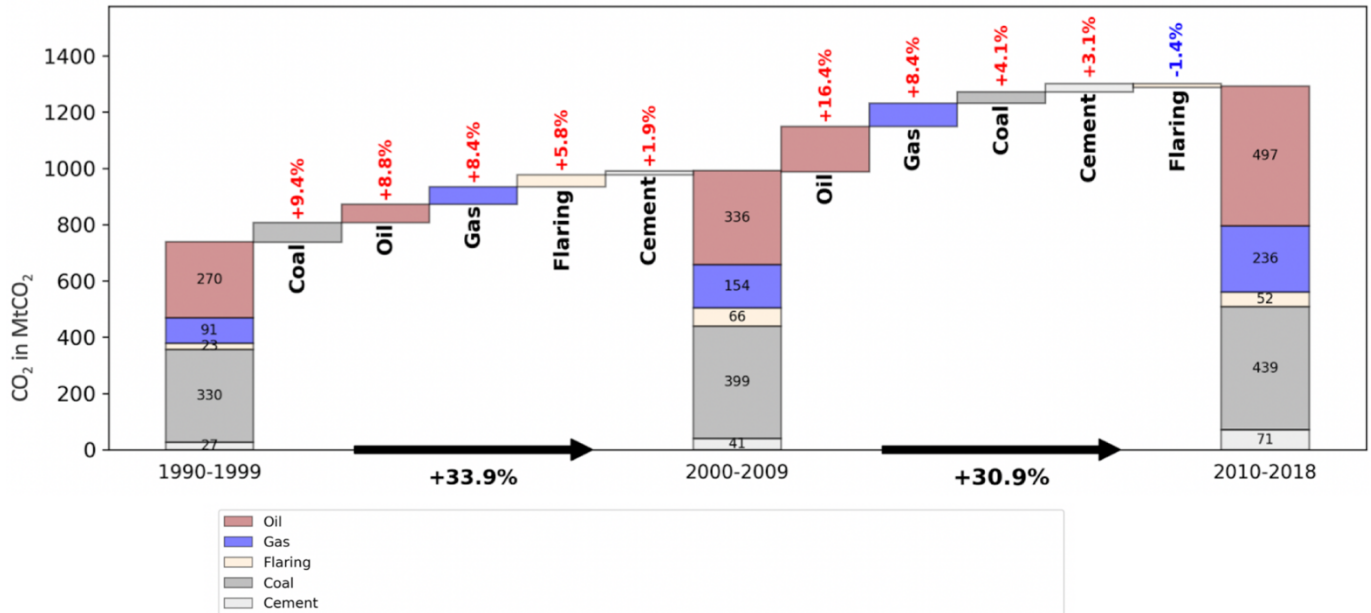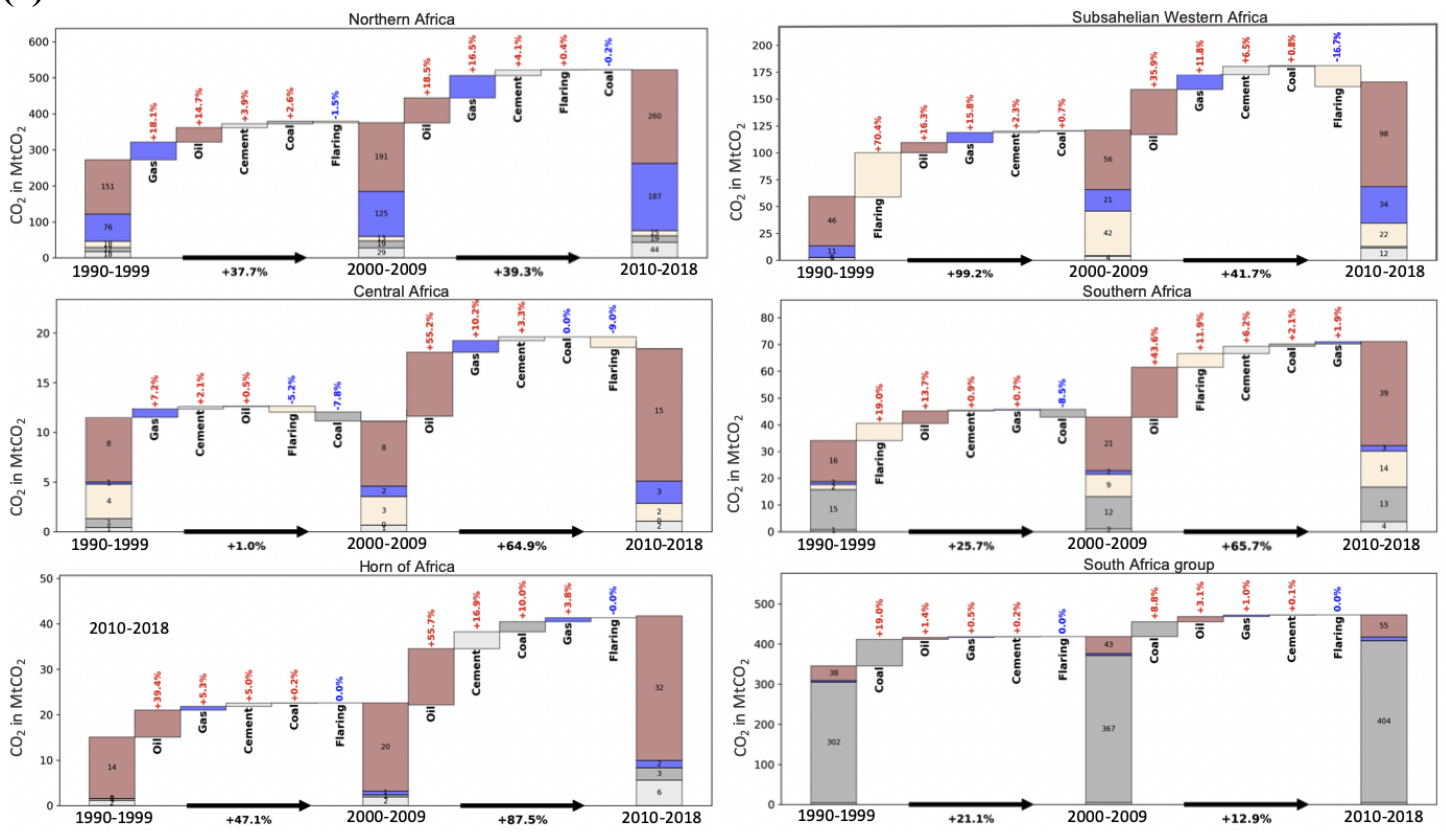
Figure 2. (a) African fossil fuel CO₂ emissions per fuel type and for cement per region over 1990-1999, 2000-2009 and 2010-2018. (b) Contribution of each fuel type to the change of African emissions. (c) Same for different regions regrouping several countries. Data from GCP (2019).

a) FCO₂ total anthropogenic emissions mean 1999-2008 in Mt yr⁻¹ (GCP).
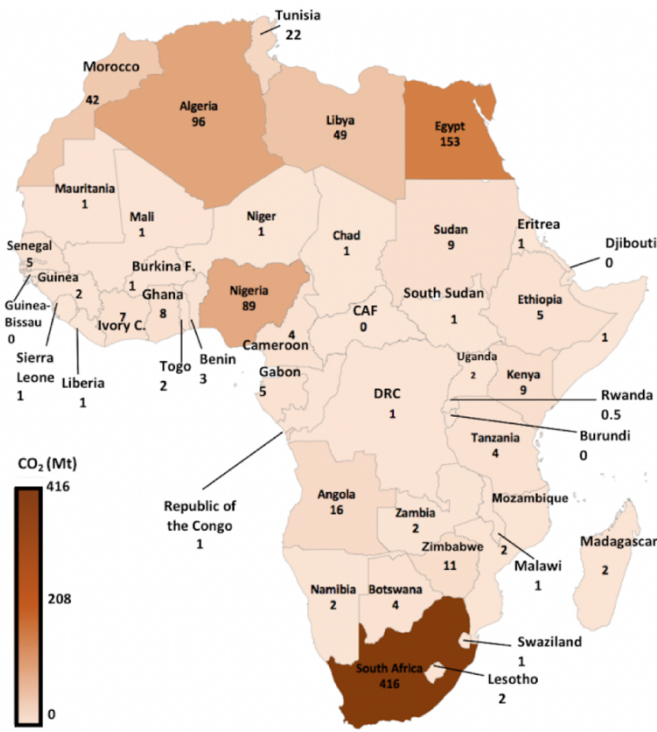
b) Differences expressions in percentage between FCO₂ total anthropogenic mean emissions 2009-2018 and mean 1999-2008 divided by average value for both decades (GCP).
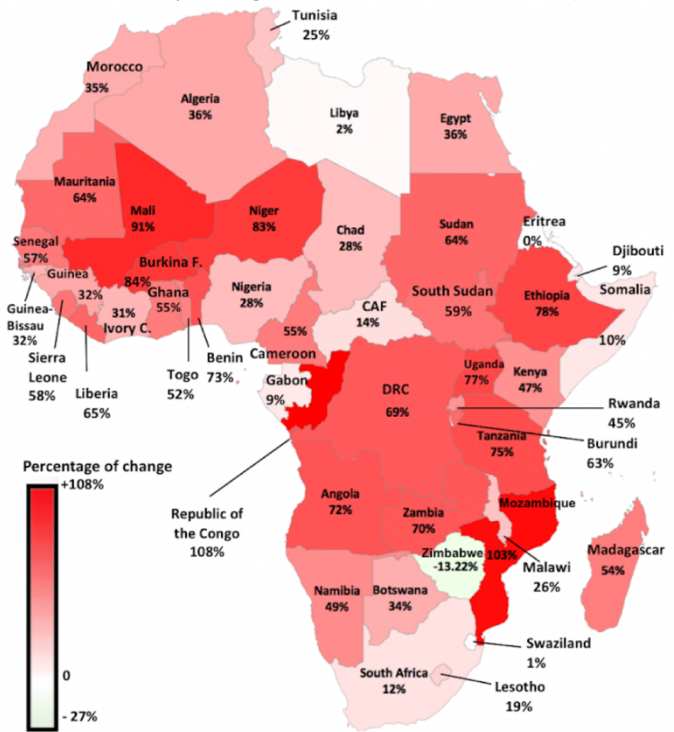
c) CH₄ total anthropogenic emissions mean 1999-2008 in MtCO₂e yr⁻¹ (PRIMAP-hist).
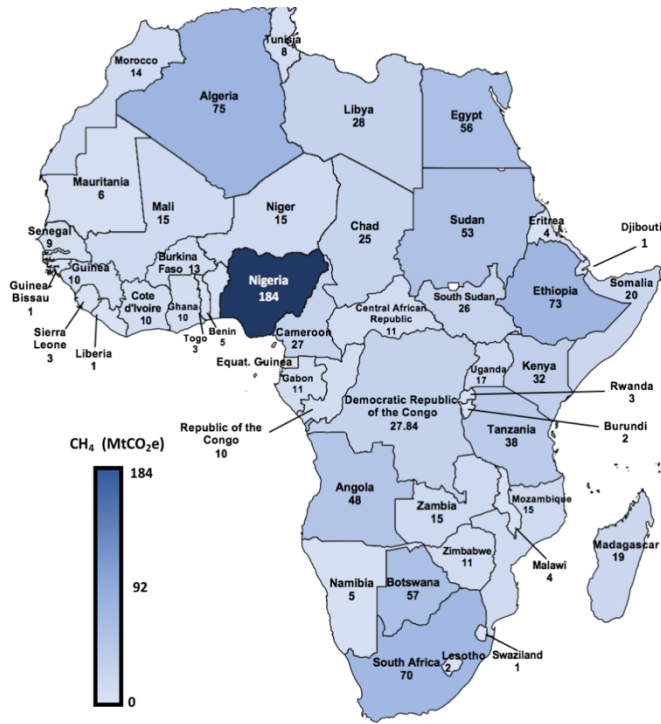
d) Differences between CH₄ total anthropogenic mean emissions 2009-2018 and mean 1999-2008 in MtCO₂e yr⁻¹ (PRIMAP-hist).
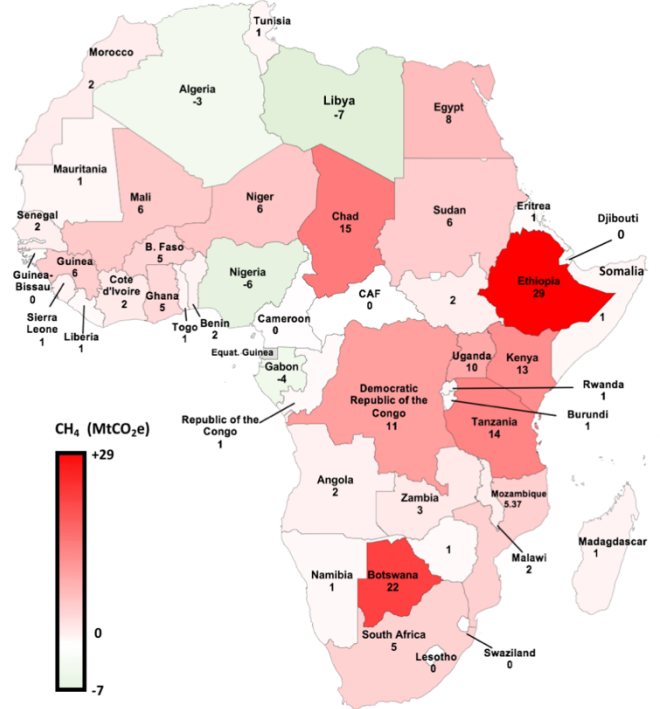
e) N₂O total anthropogenic emissions mean 1999-2008 in MtCO₂e yr⁻¹ (PRIMAP-hist).

f) Differences between N₂O total anthropogenic mean emissions 2009-2018 and mean 1999-2008 in MtCO₂e yr⁻¹ (PRIMAP-hist).
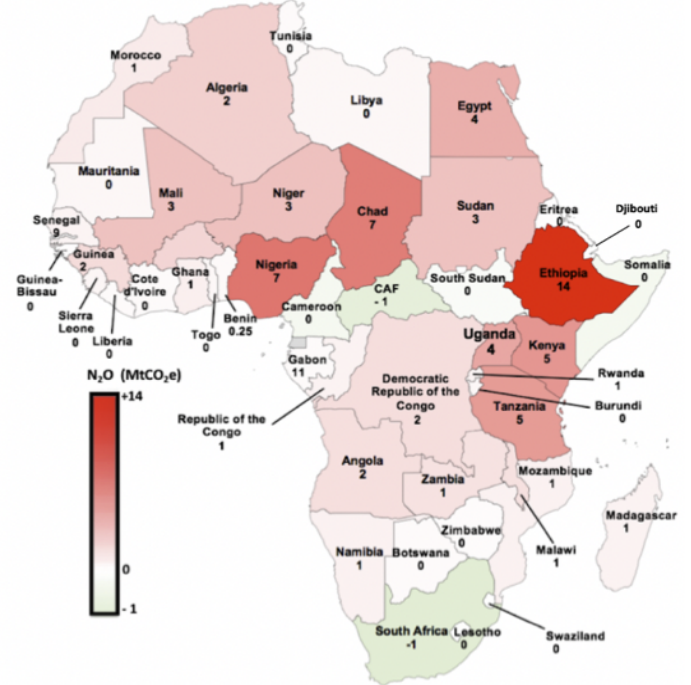
Figure 3 (a). Maps of average fossil fuel CO_2 emissions for African countries during 1999-2008 in MtCO₂e yr^{-1} and (b) change from 1999-2008 to 2009-2018 using data from GCP in MtCO₂e yr^{-1} (Friedlingstein et al., 2019); (c-d) same but with anthropogenic CH_4 emissions from PRIMAP-hist in MtCO₂e yr^{-1}; (e-f) same for anthropogenic N_2O emissions from PRIMAP-hist in MtCO₂e yr^{-1}.

PRIMAP-hist and GCP

First, we compared GCP and PRIMAP-hist fossil CO_2 emissions. We found that most of the relative differences between these two datasets at country level considerably decreased with time, except for Mali. Those differences are less than 5% for most of the main African emitters during the last decade, except for South Africa where the difference is a bit larger than 10% (see maps in Fig. S8). The largest relative difference between the two datasets comes from Mali in the decade 2009-2018, with FCO_2 emissions of 3 $MtCO_2$ yr^{-1} in GCP, compared to 1 $MtCO_2$ yr^{-1} in PRIMAP-hist. Given the relatively small differences, we chose to use only GCP for trends between decades, but when computing net budgets for the three main GHG, we show differences between the use of those two estimates.

The changes of African FCO_2 emissions per fuel type and for cement using the GCP data are shown in Fig. 2 (a). In Fig.2 (b), we show absolute values and relative contributions to the total change in each decade. During 2010-2018, total African FCO_2 emissions from oil (497 $MtCO_2$ yr^{-1}) and coal (439 $MtCO_2$ yr^{-1}) were roughly similar. While global FCO_2 emissions increased by +13 % over this period (Friedlingstein et al., 2019), African FCO_2 almost doubled in 2018 compared to 1990 levels, a relative increase comparable with that of China over the same period. From 1990-1999 to 2000-2009, the mean emissions increased by 33.9% from 741 $MtCO_2$ yr^{-1} to 996 $MtCO_2$ yr^{-1}. All FCO_2 sectors contributed to this decadal increase. The contribution from coal (+9.4 %) was slightly larger but comparable to that from oil (+9 %) and gas (+8 %). From 2000-2009 to 2010-2018, emissions further increased by 31% from 996 $MtCO_2$ yr^{-1} to 1295 $MtCO_2$ yr^{-1}. The oil and the gas fuels contributed the most to this increase with +16 % for oil, and +8 % for gas. Coal emissions increased by only +4.1 % and coal went from being the first source of African FCO_2 emissions over 2000-2009 to the second one over 2010-2018.

As for regional contributions to emissions changes between 1990-1999 and 2000-2009 shown in Fig. 2 (b) the main contribution to the total increase came from the region of South Africa where emissions increased from 302 $MtCO_2$ yr^{-1} to 367 $MtCO_2$ yr^{-1} (+21.1 %, coal being the largest contributor). The second largest contribution to the increase is from North Africa where oil was the largest contributor (emissions increased from 151 $MtCO_2$ yr^{-1} to 191 $MtCO_2$ yr^{-1}; +15 %), and gas (+18%). The least increasing region was Central Africa. North Africa

500 experienced the largest increase from 1990-1999 to 2000-2009, and from 2000-2009 to 2010-2018 with
501 successive increases of +38 % and +39 %, largely dominated by oil and gas (Fig. 4 (b)). As a result, during the
502 period 2010-2018, Northern African countries were the dominant emitters with 545 $MtCO_2$ yr^{-1}. The group of
503 South Africa (including Lesotho and Botswana) was the second biggest emitter region over 2010-2018, mainly
504 due to coal emissions from the Republic of South Africa. The two least contributing African regions were the
505 Horn of Africa and Central Africa.

506 At the country level, Figure 3a-b shows mean FCO_2 emissions and relative changes over the last two decades.
507 The main emitters do not have the biggest relative changes. The four main emitters over 2000-2009 were South
508 Africa (416 $MtCO_2$ yr^{-1}), Egypt (153 $MtCO_2$ yr^{-1}), Algeria (96 $MtCO_2$ yr^{-1}) and Nigeria (89 $MtCO_2$ yr^{-1}). Those
509 four countries altogether represented 67% of the continental total emissions over 2000-2009 (987 $MtCO_2$ yr^{-1}).
510 The largest relative increases from 2000-2009 to 2010-2018 are from Congo (+108 %), Mozambique (+103 %)
511 and Mali (91%), compared to relative increases in the main emitters, the Republic of South Africa (+21 %),
512 Egypt (+36%) and Algeria (+36%).
513
514 **2.1.2 Variations of per capita and per GDP fossil fuel CO_2 emissions**
515
516 **Per capita emissions**

517 Using ancillary data on population (Fig. S3and Fig. S4) we computed the mean African per capita emissions
518 of 1 tCO_2/cap yr^{-1} for 2009-2018, which is 5 times larger than during 1990-1998 (0.2 tC/cap yr^{-1}), and yet 5
519 times smaller than the global average (5 tCO_2/cap yr^{-1}). From 1999-2008 to 2009-2018, African per capita
520 emissions increased by 30 %. African per capita FCO_2 emissions during 2009-2018 were 17 times less than in
521 the USA (17 tCO_2/cap yr^{-1}), 7 times less than in China (7 tCO_2/cap yr^{-1}), 7 times less than in EU27+UK (7
522 tCO_2/cap yr^{-1}), and 2 time less than India (2 tCO_2/cap yr^{-1}). At the country level, the biggest per capita emissions
523 over 2009-2018 were from the Republic of South Africa with 9 tCO_2/cap yr^{-1}, which ranks 14th worldwide,
524 above China and just below Poland. The second biggest per capita emissions were from Libya (8 tCO_2/cap yr^{-}
525 ^{1}). The smallest ones were from the DRC (0.1 tCO_2/cap yr^{-1}). For the first period 1990-1998, per capita
526 emissions of African region ranked in this order: South Africa group (4 tCO_2/cap yr^{-1}) > Northern Africa (2
527 tCO_2/cap yr^{-1}) > Central African countries (1 tCO_2/cap yr^{-1}) > Southern countries (0.8 tCO_2/cap yr^{-1}) > Horn of
528 Africa (0.5 tCO_2/cap yr^{-1}) > Sub-Sahelian Western Africa (0.3 tCO_2/cap yr^{-1}). For the second period 2009-2018,
529 they ranked in this order: South Africa group (4 tCO_2/cap yr^{-1}) > Northern Africa (2 tCO_2/cap yr^{-1}) > Southern
530 countries (1 tCO_2/cap yr^{-1}) and Horn of Africa (1 tCO_2/cap yr^{-1}) > Central Africa countries (1 tCO_2/cap yr^{-1}) >
531 Sub-Sahelian Western Africa (0.4 tCO_2/cap yr^{-1}). At country scale during the first period of 1990-1998, the

532   four African largest per capita emissions ranked in this order: Libya (9 tCO_2/cap yr^{-1} > the Republic of South

533   Africa (9 tCO_2/cap yr^{-1}) > Gabon (5 tCO_2/cap yr^{-1}) > Algeria (3 tCO_2/cap yr^{-1}). The four African countries with

534   the smallest per capita emissions ranked as following: Burundi (0.04 tCO_2/cap yr^{-1}) < Uganda, Ethiopia and

535   Mali (0.1 tCO_2/cap yr^{-1}).

536   We also computed the GINI index for African per capita FCO_2 emissions for each of the last three decades,

537   using data from (Friedlingstein et al., 2020) (see Methodological Supplementary M2). These GINI values were

538   0.7 for 1990-1998, 0.7 for 1999-2008, and 0.7 for 2009-2018, thus very stable over the last 30 years and close

539   to 1, indicating high inequities among countries.

540   **Emissions per GDP**

541   **Per exchange rate vs. per Purchasing Power Parities (PPP) GDP**

542   According to the International Monetary Fund (IMF), the Gross Domestic Product (GDP) delivers an estimate

543   "of the monetary value of goods and services produced in a country over a chosen period." GDP data from the

544   World Bank (2015) is available for 30 African countries only (Fig. S5). The four countries with the biggest per

545    $US exchange rate GDP (Fig. S6) are: Nigeria ($490 B) > South Africa ($350B) > Egypt ($330B) and Algeria

546   ($330B) > Angola ($120B). The four countries with the smallest GDP in 2015 are: Gambia ($1.4B) and

547   Seychelles ($1.4B) > Guinea-Bissau ($1B) > Comoros ($970 M). Emissions per $US GDP are shown in Fig.

548   S6 The Purchasing Power Parities (PPP) calculated by the International Comparison Program (ICP) of the

549   World Bank is a refined measure of what a given national currency can acquire in terms of goods or services

550   in another country, removing the impact of currency exchange rates. Emissions per PPP$ GDP are shown in

551   Fig. S7.

552   The mean of African emissions per unit PPP$ GDP in 2016 was 0.6 $kgCO_2$/PPP$ yr^{-1}, which is more than twice

553   the global value, 3 times the mean value of the USA (0.2 $kgCO_2$/PPP$ yr^{-1}), and Europe (0.2 $kgCO_2$/PPP$ yr^{-1}

554    $^{-1}$). This points to a more carbon intensive economic growth in Africa than in developed countries, which may

555   be an important barrier for future mitigation strategies as the GDP of Africa has grown by 112% in the last 30

556   years, and is projected to increase in the future by 3% per year (World Bank, 2022). At regional level, the

557   largest values were: South Africa (0.4 $kgCO_2$/PPP$ yr^{-1}) > North Africa, Southern Countries and Sahelian

558   Western Africa (0.2 $kgCO_2$/PPP$ yr^{-1}) > Central Africa and the Horn of Africa (0.1 $kgCO_2$/PPP$ of GDP). At

559   country scale, the largest emitters per unit of GDP were Libya (0.7 $kgCO_2$/PPP$ yr^{-1}) and South Africa (0.7

560    $kgCO_2$/PPP$ yr^{-1}) > Lesotho (0.4 $kgCO_2$/PPP$ yr^{-1}) > Algeria (0.3 $kgCO_2$/PPP$ yr^{-1}) (Fig. S7.) The smallest

561   emitters were: DRC (0.03 $kgCO_2$/PPP$ yr^{-1}) < Chad (0.04 $kgCO_2$/PPP$ yr^{-1}) < Burundi (0.06 $kgCO_2$/PPP$ yr^{-1}

562    $^{-1}$) < Uganda (0.07 $kgCO_2$/PPP$ yr^{-1}).

563 We also used GDP per unit exchange rate from the International Energy Agency (IEA, 2019). The mean African

564 emissions per unit of $GDP_{exch.rate}$ was 0.5 $kgCO_2$ $_{\$}$/$ yr^{-1}, larger than elsewhere, except in Asia (0.6 $kgCO_2$/

565 $GDP_{exch.rate}$ yr^{-1}. As shown in Fig. S6, over 2013-2017 the six biggest emitters were South Africa (0.7 $kgCO_2$/

566 $GDP_{exch.rate}$ yr^{-1}) > Libya (0.5 $kgCO_2$/ $GDP_{exch.rate}$ yr^{-1}) > South Sudan (0.4 $kgCO_2$/ $GDP_{exch.rate}$ yr^{-1}) > Zimbabwe,

567 Benin and Algeria (0.3 $kgCO_2$/ $GDP_{exch.rate}$ yr^{-1}). The correlation coefficient between $GDP_{exch.rate}$ and FCO_2

568 emissions per $GDP_{exch.rate}$ was 0.3, suggesting that the countries with a high GDP do not always emit more CO_2

569 per unit GDP. For instance, South Africa ranked first with 0.7 $kgCO_2$/ $GDP_{exch.rate}$ yr^{-1} and second for GDP (350

570 $Billion); Nigeria ranked first for GDP (490 $Billion), but 21st for emissions per GDP (0.1 $kgCO_2$/ $GDP_{exch.rate}$

571 yr^{-1}). This may be related to the fact that countries with a high GDP are also more likely to create growth

572 through sustainable activities.

573

574 **2.2 LULUCF CO_2 fluxes**

575 **Outlier corrections**

576 (a)
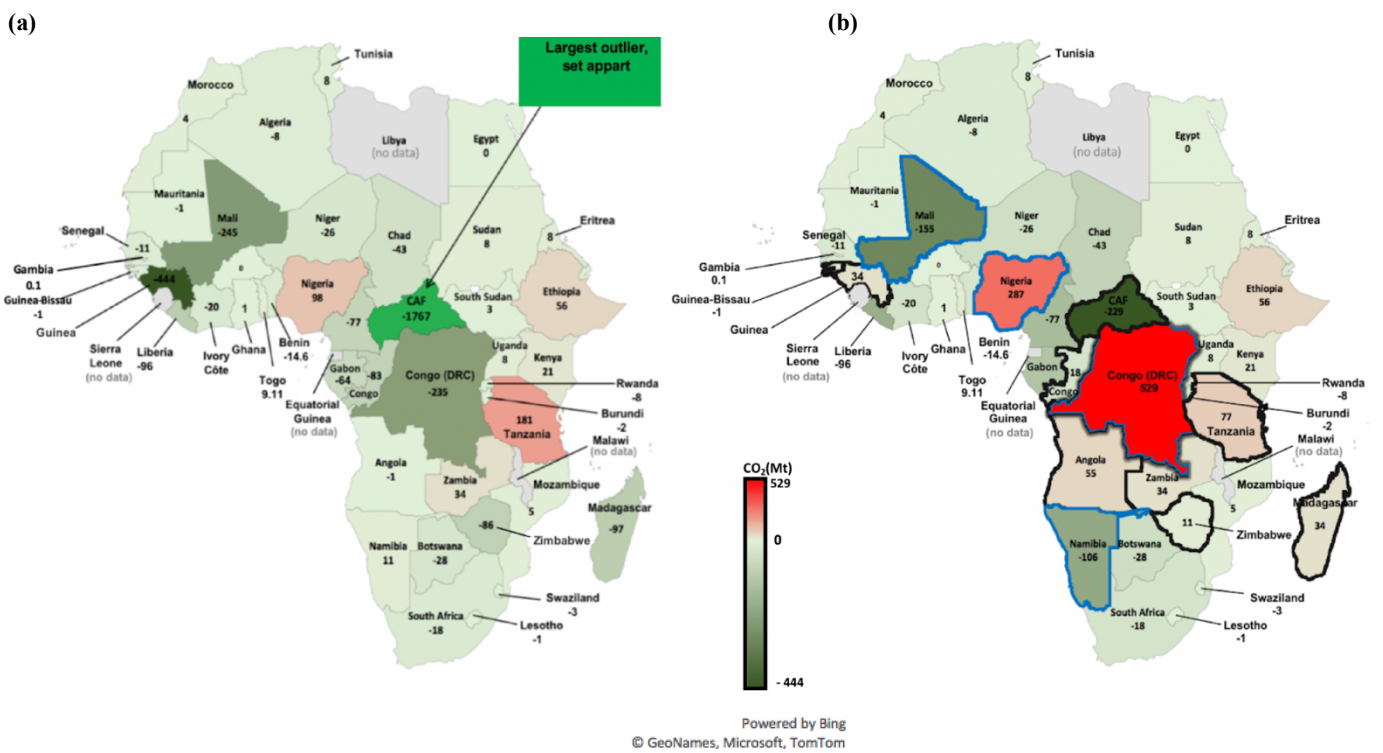
577
578
579
580
581
582
583
584
585
586
587
588

589

590
591

592
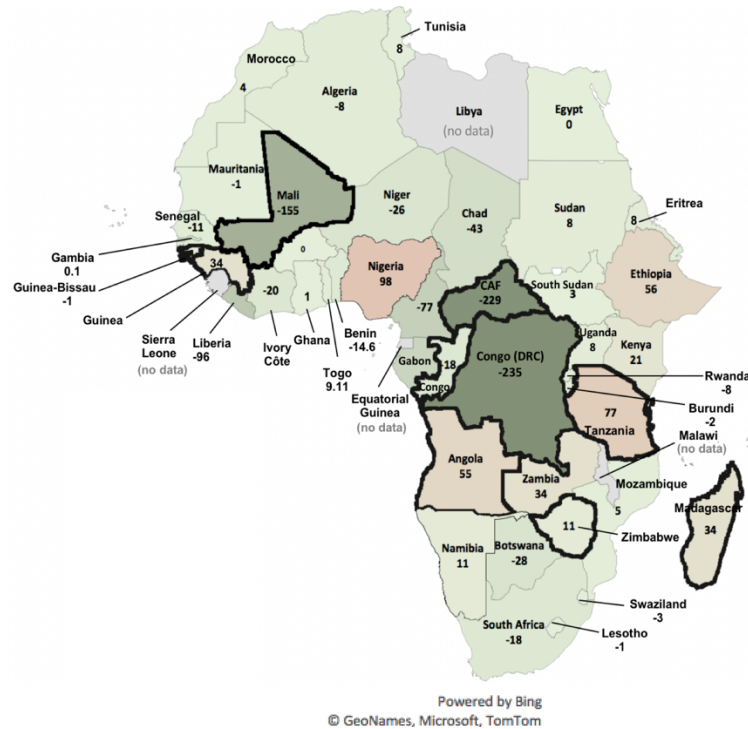
593   **Figure 4. Map of national LULUCF CO_2 fluxes for 2001-2018 in MtCO$_2$ yr^{-1}. (a) Before outliers' removals.**
594   **(b) After outliers' removal according to Grassi et al. (2022). (c) After outlier removals (DRC, Namibia and**
595   **Nigeria) from this study. Positive values represent a net C loss by ecosystems.**

596
597   In this section, we analyze CO_2 fluxes from the LULUCF sector, based on UNFCCC data (section 1.1)
598   which include forest lands, grasslands, croplands, and all possible conversions between them (IPCC,
599   2003; 2006). As shown in section 1.2 and Table S4, we found that some countries' reports are outliers
600   with biophysically implausible CO_2 sinks and/or sudden unexplained very large changes between
601   successive reports. Due to scarce data over 1990-1998 we focus on the period 2001-2018. In the
602   following paragraph, we discuss four approaches to include UNFCCC data:

603   a) Uncorrected data, b) corrections following Grassi et al. (2022) for all countries, c) corrections
604   following Grassi et al. (2022) except DRC, Namibia and Nigeria, d) Corrections following Grassi et al.
605   (2022) except for DRC.

606   Figure 4 (a) shows UNFCCC data without correcting for outliers, based on BUR and NC data accessed
607   in May 2022. The majority of countries are sinks, or small sources, except Tanzania and Nigeria being
608   large sources. Very large (implausible) sinks are seen in Guinea and CAF. The continent is a CO_2 sink
609   of -3309 MtCO$_2$ yr^{-1} during the period 2001-2018.

Figure 4 (b) shows the corrected fluxes according to Grassi et al. (2022) who excluded implausible large sink rates and used NDC and REDD+ reports instead of NC data for DRC, Congo, CAF, Guinea, Madagascar and the most recent BUR, NC and inventory data for Namibia, Angola, Zimbabwe and Nigeria (see their Table 7). Africa as a whole is a CO_2 source of 265 $MtCO_2$ yr^{-1}. At regional scale, the mean CO_2 sources distributes as follows on four regions: Sub-Sahelian West Africa (235 $MtCO_2$ yr^{-1}) > Horn of Africa (153 $MtCO_2$ yr^{-1}) > Central Africa (144 $MtCO_2$ yr^{-1}) > Southern Africa (14 $MtCO_2$ yr^{-1}). The two sink regions are North Africa (-259 $MtCO_2$ yr^{-1}) and South Africa (-23 $MtCO_2$ yr^{-1}). At country scale, after the corrections of Grassi et al. (2022), the four countries with the larger sinks are: CAF (-229 $MtCO_2$ yr^{-1}) > Mali (-155 $MtCO_2$ yr^{-1}) > Namibia (-106 $MtCO_2$ yr^{-1}) > Cameroon (-77 $MtCO_2$ yr^{-1}). The four countries with largest sources are DRC (529 $MtCO_2$ yr^{-1}) > Nigeria (287 $MtCO_2$ yr^{-1}) > Tanzania (77 $MtCO_2$ yr^{-1}) > Ethiopia (56 $MtCO_2$ yr^{-1}). A main issue with the correction from Grassi is that it reports no sink in DRC which has an important forest coverage representing 68% of the country area (FAO, 2015) and for which a sink was consistently reported in previous NCs.

Figure 4 (c) shows LULUCF CO_2 in African countries that are consistent with Grassi et al. (2022) except for three countries: Namibia (we used 2000 NC3 instead of NIR2019), Nigeria (we used 2014 NC2 instead of 2017 BUR2) and DRC (we used 2015 NC3 instead of 2021 NDC). In that approach Africa becomes a net CO_2 sink of -589 Mt yr^{-1} over 2001-2018. At regional scale, the region of Central Africa (-620 $MtCO_2$) remains the main sink. But the values and ranking of the top sources rank as: Horn of Africa (153 $MtCO_2$) > Southern Africa (141 $MtCO_2$) > Sub-Sahelian West Africa (19$MtCO_2$). At country scale with this correction choice, the top sinks are: DRC (-235 $MtCO_2$) > CAF (-229 $MtCO_2$) > Mali (-155 $MtCO_2$); and the three top sources: Nigeria (98 $MtCO_2$) > Tanzania (77 $MtCO_2$) > Ethiopia (56 $MtCO_2$).

In the fourth approach where we use the corrections of Grassi et al. (2022) except for DRC where we kept the latest national communication instead of the most recent NDC, the continent is a net sink of -504 $MtCO_2$ yr^{-1} over 2001-2018. At regional scale, Central Africa is a large CO_2 sink, and the ranking of sink regions is: Central African group (-620 $MtCO_2$ yr^{-1}) > North Africa (-259 $MtCO_2$ yr^{-1}) > South Africa (-23 $MtCO_2$ yr^{-1}). The ranking of the source regions stays unchanged. At the country scale, the main sink is DRC (-235 $MtCO_2$ yr^{-1}). In the paper, we will mainly use data corrected following Grassi et al. (2022), but we want to raise a caution flag that adopting their correction for DRC had an enormous effect on the CO_2 budget of the continent, which becomes a source. Using the original latest national communication of DRC instead of the NDC used by Grassi et al., and our own corrections for Namibia and Nigeria instead of those of Grassi et al. increased the continental CO_2 uptake.

Comparison of UNFCCC managed land area and FAO forest and other wooded lands areas

Figure S10 shows a comparison of land areas reported in NC, BUR and REDD+ reports (https://redd.unfccc.int/submissions.html?mode=browse-bycountry) with FAO forest land areas (2015) and FAO forest land + other woodlands areas for the year 2015 (see Table S9). Consistent with Grassi et al. (2022), all forest lands in Africa are considered as managed. We found that FAO forest lands areas are closer to UNFCCC estimates than the sum of FAO forest and other woodlands area, except for DRC, Sudan, Senegal, Niger and Mauritania (Table S9). Forest areas in UNFCCC data using IPCC default method do not exactly match FAO data estimates of forest area.

LULUCF CO$_2$ fluxes from UNFCCC versus DGVM and inversions

A comparison between LULUCF CO$_2$ fluxes from UNFCCC, FAO, DGVMs and inversions is shown in Fig. 5 at the scale of the continent and for the six regions. The period of overlapping time series is 2001-2018. For the continent, DGVMs give a mean sink of -232 MtCO$_2$ yr^{-1} with a huge range from -1977 MtCO$_2$ yr^{-1} to 2095 MtCO$_2$ yr^{-1}. The years with the biggest sinks for DGVM (from the median of all models) are 2006 and 2018, and the years with the smallest sinks are 2005 and 2016 which seem related to widespread drought years across Africa. A key result shown by this figure is that the DGVMs and inversions show a huge spread, making them of little value to 'verify' inventories for LULUCF CO$_2$ fluxes in Africa. Yet, we observed that the median of all DGVM points to a sink for Africa, unlike the UNFCCC data with the correction from Grassi et al. (2022).
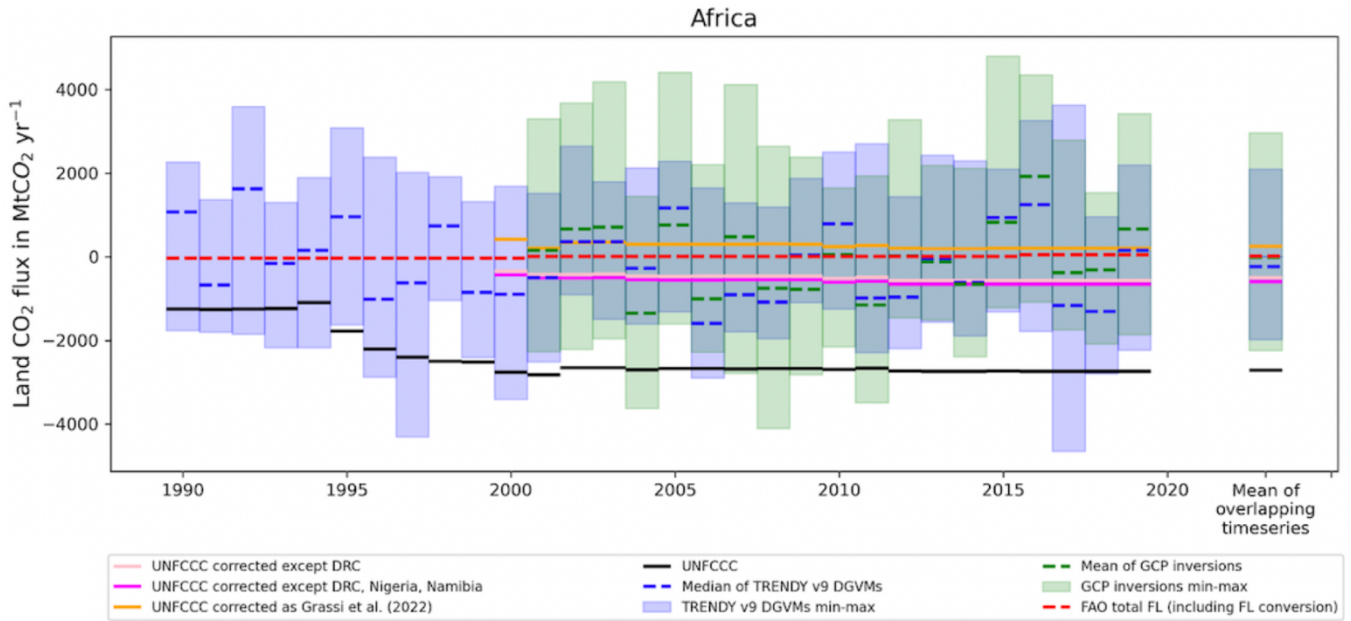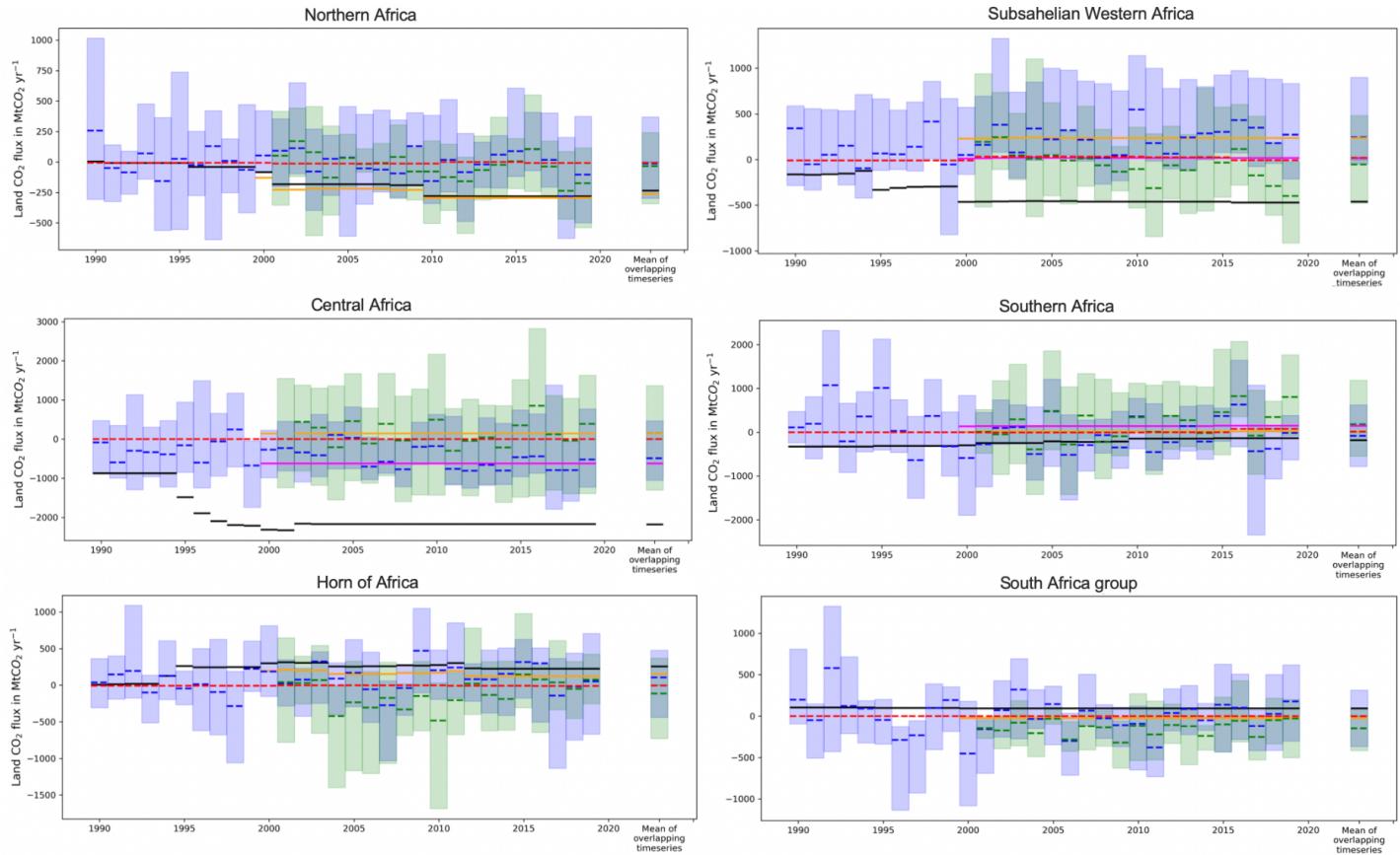
Figure 5. LULUCF CO₂ emissions and sinks: comparison between UNFCCC national greenhouse gas inventories, TRENDYv9 DGVMs and inversions, for total Africa and for each of the six African sub regions; as well as country details for the three lain outliers. The unit is in MtCO₂ yr⁻¹ Shaded green areas represent the minimum and maximum ranges from inversions. Shaded blue represents the minimum and maximum ranges for TRENDYv9 DGVMs. Green dashes denote the mean of inversions, blue dashes denote the median of TRENDYv9 DGVMs, green dashes the median of inversions. Positive values represent a source while the negative values refer to a sink.

For three large countries, corrected UNFCCC values from Grassi et al. show a bigger discrepancy with other BU and TD methods than uncorrected ones (Fig. S9). In Namibia the corrected value gives a larger sink compared to other methods, while the uncorrected value is comparable. In DRC the corrected value which was a source seems a high overestimate compared to other methods, while the uncorrected UNFCCC value is close to median values from inversions, and to FAO. In Nigeria, the corrected value seems to be a high overestimation of a net source compared to other methods pointing to either a smaller source (FAO, inversions) or even a sink (DGVM).

The data in Figure 5 show that most methods agree on a small net sink for African LULUCF CO_2 fluxes, except for corrections following Grassi et al (2022). But disagreements exist among different methods. Inversions give a smaller net sink ($\text{mean}_{\min}^{\max}$) of -14 $_{-2\,248}^{2\,966}$ $MtCO_2$ yr^{-1} than DGVMs (-232 $_{-1978}^{2095}$ $MtCO_2$ yr^{-1}). The median value of inversions is nevertheless within the range of DGVMs. At the scale of Africa, the inversions mean sink is ∼12 times smaller than the median from DGVMs. The min-max range of inversions (5216 $MtCO_2$ yr^{-1}) is larger than the range of the DGVMs by 17%. DGVM and inversions show a positive temporal correlation coefficient ($r = 0.7$) for annual trends (linear fit to time series).

UNFCCC values with the fourth approach point out to a net sink (-503 $MtCO_2$ yr^{-1}), similar to the third one. Corrected values as in Grassi et al. (2022) give a net source estimate of 265 $MtCO_2$ yr^{-1}. FAO net emissions and removals represent a small net source (18 $MtCO_2$ yr^{-1}). Differences between FAO and UNFCCC, as explained in Grassi et al. (2022), could be due to the fact that FAO estimates of CO_2 fluxes for forest remaining forest can be set to zero in absence of any national stock change inventory (Table 3).

Table 3. Mean net LULUCF CO_2 (emissions and removals) over the overlapping period of the different datasets (2001-2018), in $MtCO_2$ yr^{-1}.

Region	Corrected UNFCCC (Grassi et al. 2022) with and without DRC correction.	Corrected UNFCCC but DRC/ Nigeria/ Namibia	Median TRENDY v9	Max TRENDY v9	Min TRENDY v9	Mean GCB inv.	Max GCB inv.	Min GCB inv.	FAO total FL with FL conversion
South Africa group	-23	-23	-5	312	-368	-147	96	-418	-1
Horn of Africa	153	153	108	475	-439	-115	367	-729	-5
Southern Africa	14	**141**	-81	622	-785	182	1186	-548	13
North Africa	-259	-259	-13	369	-299	-34	240	-343	-9
Subsahelian West Africa	236	**19**	245	900	-49	-53	481	-479	21
Central Africa	**144** (DRC with NDC2021) **-620** (DRC with NC3)	-620	-490	461	-1051	152	1362	-1303	-1
Africa total	**265** (DRC with NDC2021) **-503** (DRC with NC3)	-589	-232	2095	-1978	-14	2967	-2249	-1

696   At a regional scale, we note some agreement between different BU approaches. First, for the South Africa

697   region, the mean of DGVM medians during the overlapping period 2001-2018 (-5 $MtCO_2$ yr^{-1}) and the

698   FAO estimate (-1 $MtCO_2$ yr^{-1}) are comparable and not too far from Grassi et al., 2022 (-23 $MtCO_2$ yr^{-1}).

699   Second, for North Africa, the DGVM median (-13 $MtCO_2$ yr^{-1}) and the FAO mean estimate over the same

700   period (-9 $MtCO_2$ yr^{-1}) are comparable. Finally, in Sub-Sahelian West Africa, the DGVM (236 $MtCO_2$ yr^{-1})

701   ) and UNFCCC corrected following Grassi et al., 2022 (245 $MtCO_2$ yr^{-1}) are also close to each other.

702

703   Northern Africa is the group where DGVM and inversions point to the closest values both in terms of sign

704   (sink) and magnitudes with respectively small sinks of -13^{369}_{-299} $MtCO_2$ yr^{-1} and -34^{240}_{-343} $MtCO_2$ yr^{-1}.

705   Looking at DGVM and inversions in the region of South Africa, we found that both DGVM and inversions

706   point to a sink (respectively -5^{312}_{-368} $MtCO_2$ yr^{-1} and -147^{96}_{-418} $MtCO_2$ yr^{-1}), however with a different

707   magnitude. The region showing the highest discrepancies between inversions and DGVM values is Central

708   Africa with a source in inversions (152^{1362}_{-1303} $MtCO_2$ yr^{-1}) and a sink for DGVM (-490^{461}_{-1051} $MtCO_2$ yr^{-1}).

709   The Sub-Sahelian West Africa also shows discrepancies in both sign and magnitude with 245^{900}_{-49} $MtCO_2$

710   yr^{-1} for DGVM and -53^{481}_{-479} $MtCO_2$ yr^{-1} for inversions. The same is true for Southern Africa with

711   -81^{622}_{-785} $MtCO_2$ yr^{-1} for DGMVs and 182^{1186}_{-548} $MtCO_2$ yr^{-1} for inversions, and the Horn of Africa

712   with 108^{475}_{-439} $MtCO_2$ yr^{-1} for DGVM and -115^{367}_{-729} $MtCO_2$ yr^{-1} for inversions. At the regional scale, the

713   inversions systematically give smaller sinks than DGVMs in the regions of Central Africa, Sub-Sahelian

714   West Africa and North Africa after 2010 (Fig. 5).

715

716   We also computed the coefficient of correlation at the regional level between DGVM and inversions trends

717   for each region. The highest correlation coefficients are in the South Africa region (r = 0.7), followed by

718   Northern Africa (r = 0.6) and in Southern Africa (r = 0.5). The lowest correlation coefficients are for the

719   group of Central African countries (r = 0.3), Sub-Sahelian Western countries (r = 0.2) and the Horn of

720   Africa (r = 0.1).

721

722   **2.3 CH_4 anthropogenic emissions**

723   **Total and sectoral bottom up CH_4 anthropogenic emissions and decadal changes**

724

725

726

727

728   **(a)**
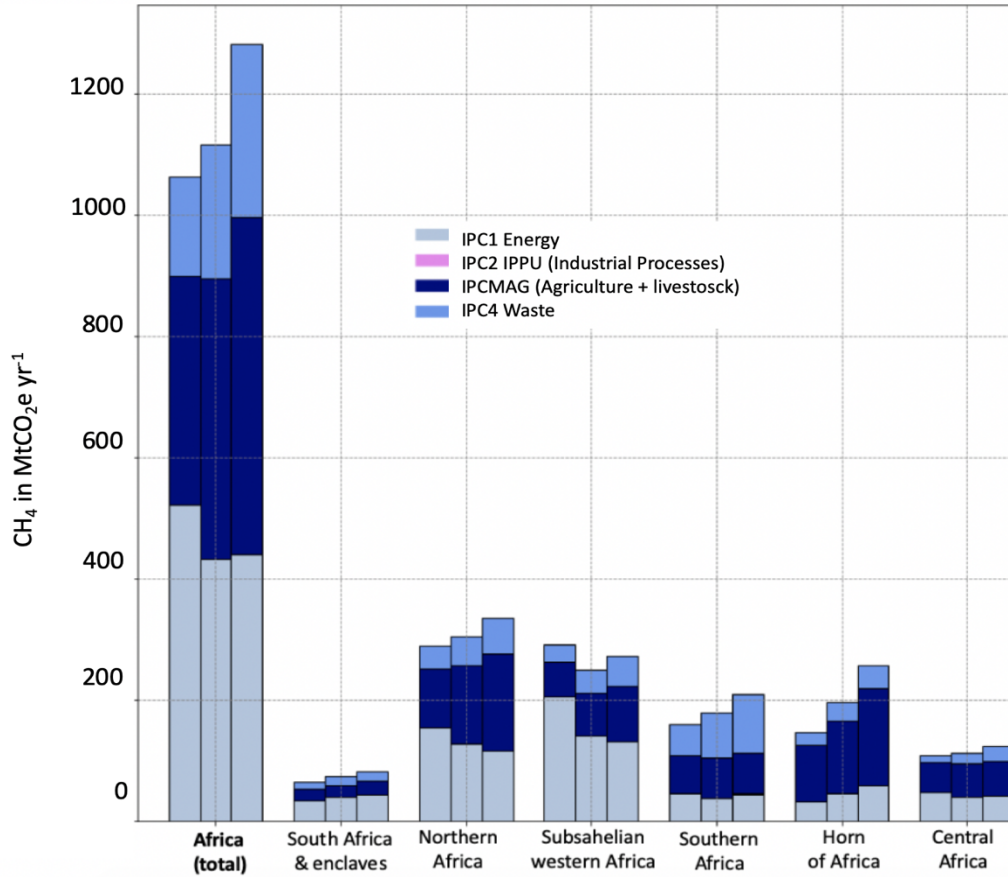
729
730   **(b)**
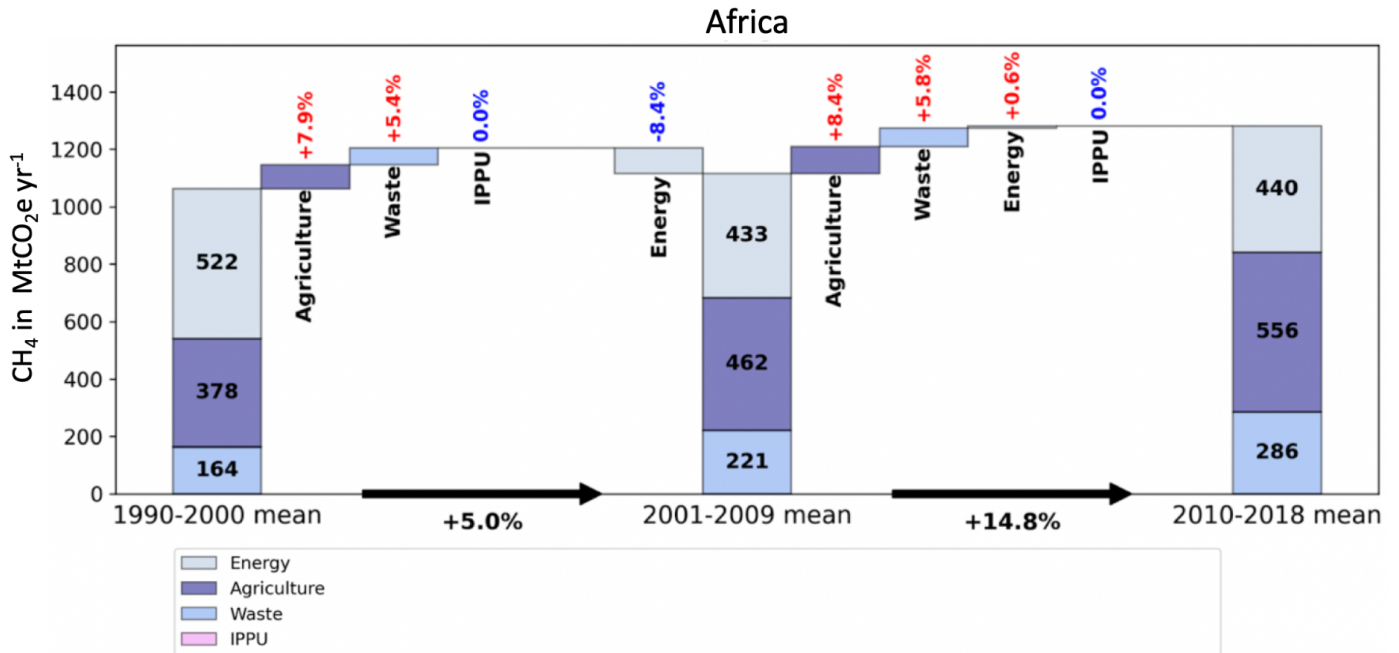
731

(c)
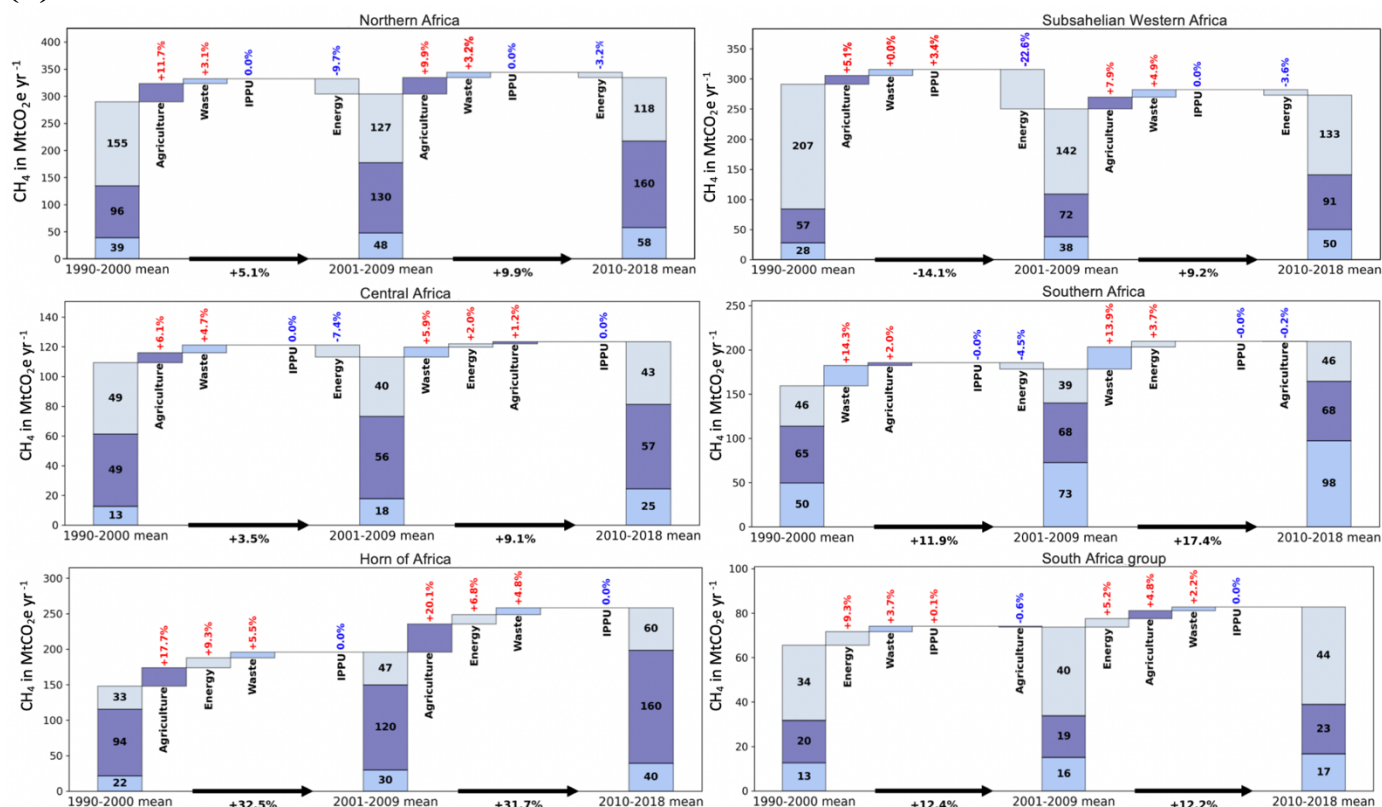
Figure 6. (a) African mean anthropogenic CH_4 emissions in $MtCO_2e$ yr^{-1} over three decades (1990-1998, 1999-2008, 2010-2018). (b) Contribution of each sector to the change of African emissions between the last three decades. (c) Same for different regions regrouping several countries. Data from PRIMAP-hist (2021).

Figure 6 shows anthropogenic CH_4 emissions from PRIMAP-hist grouped into four super-sectors (see section 1). A map of CH_4 emissions and their trends per country is given in Fig. 3c-d. LULUCF CH_4 emissions are not considered in PRIMAP-hist. African anthropogenic CH_4 emissions sum up to 1154 $MtCO_2e$ yr^{-1} over the last three decades. They increased from 1064 $MtCO_2e$ yr^{-1} in 1990-2000 to 1116 $MtCO_2e$ yr^{-1} in 2001-2009, and further to 1282 $MtCO_2e$ yr^{-1} over 2010-2018 (Fig. 6.a.) Over the last three decades, the main African CH_4 emitting super-sectors shifted from Energy (49% over 1990-2000) to Agriculture, mainly due to a North African contribution. At the regional level, the main contributing region to total emissions shifted over the last 30 years from Sub-Sahelian Western Africa (297 $MtCO_2e$ yr^{-1} for all sectors in 1990-2000) to North Africa (333 $MtCO_2e$ yr^{-1} for all sectors in 2010-2018).

North African emissions increased from 290 $MtCO_2e$ yr^{-1} in 1990-2000 to 305 $MtCO_2eq$ yr^{-1} in 2001-2009, and further to 333 $MtCO_2e$ yr^{-1} in 2010-2018. Sub-Sahelian emissions decreased from 297 $MtCO_2e$ yr^{-1} in 1990-2000 to 252 $MtCO_2e$ yr^{-1} in 2001-2009, and re-increased to 274 $MtCO_2e$ yr^{-1} in 2010-2018, a level smaller than in the first decade (Fig. 6b). The Horn of Africa emissions increased from 149 $MtCO_2e$ yr^{-1} over 1990-2000, to

197 MtCO$_2$e yr^{-1} over 2001-2009, and further to 260 MtCO$_2$e yr^{-1} over 2010-2018. The emissions from Southern Africa increased from 184 MtCO$_2$e yr^{-1} in 1990-2000, to 180 MtCO$_2$e yr^{-1} in 2001-2009, and further to 212 MtCO$_2$e yr^{-1} in 2010-2018. Emissions from the Central African region increased from 111 MtCO$_2$e yr^{-1} in 1990-2000, to 114 MtCO$_2$e yr^{-1} in 2001-2009, and further to 125 MtCO$_2$e yr^{-1} in 2010-2018. We also computed the GINI of African countries anthropogenic CH$_4$ per capita emissions and obtained the following values: 0.6 in 1990-1998, 0.5 in 1999-2008, 0.5 in 2009-2018, thus a trend of increasing 'inequality' between countries. As compared to per capita FCO$_2$ emissions, more homogeneity is observed for CH$_4$ per capita emissions. Similar to FCO$_2$ emissions, the GINI values remained stable over the three decades, showing a similar level of inequalities over time.

BU versus inversions for total and anthropogenic CH$_4$ emissions
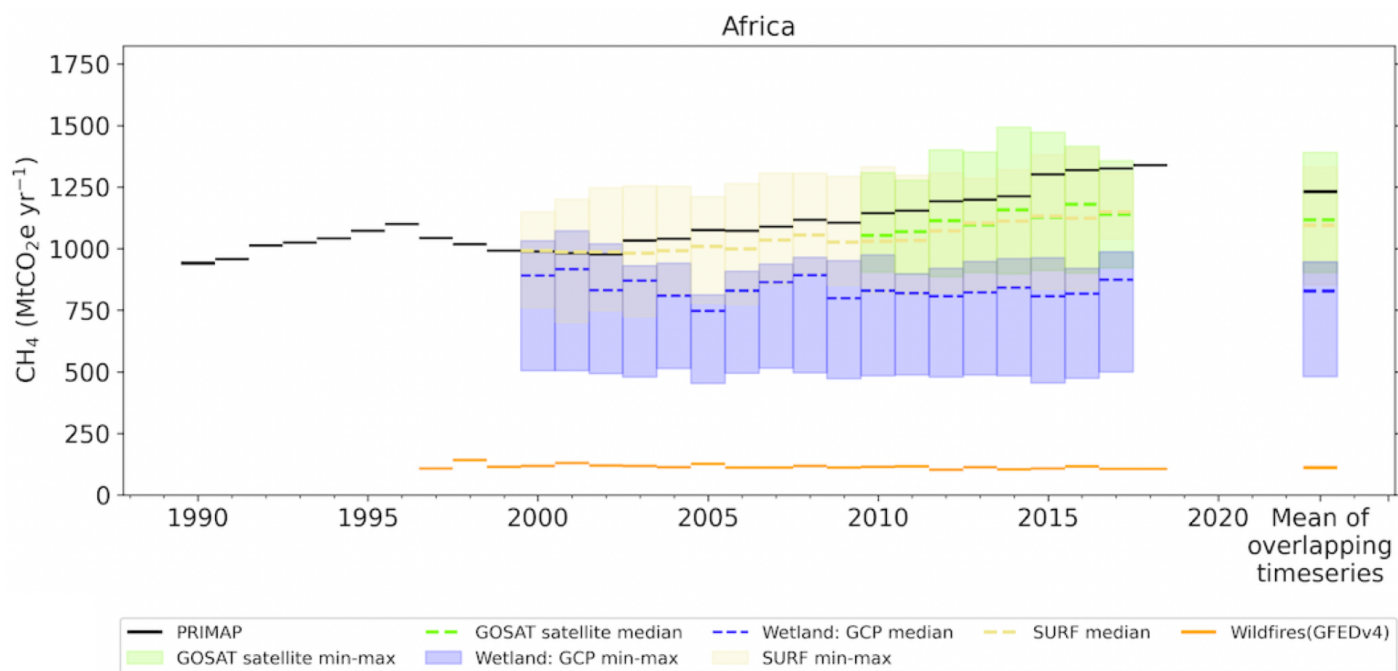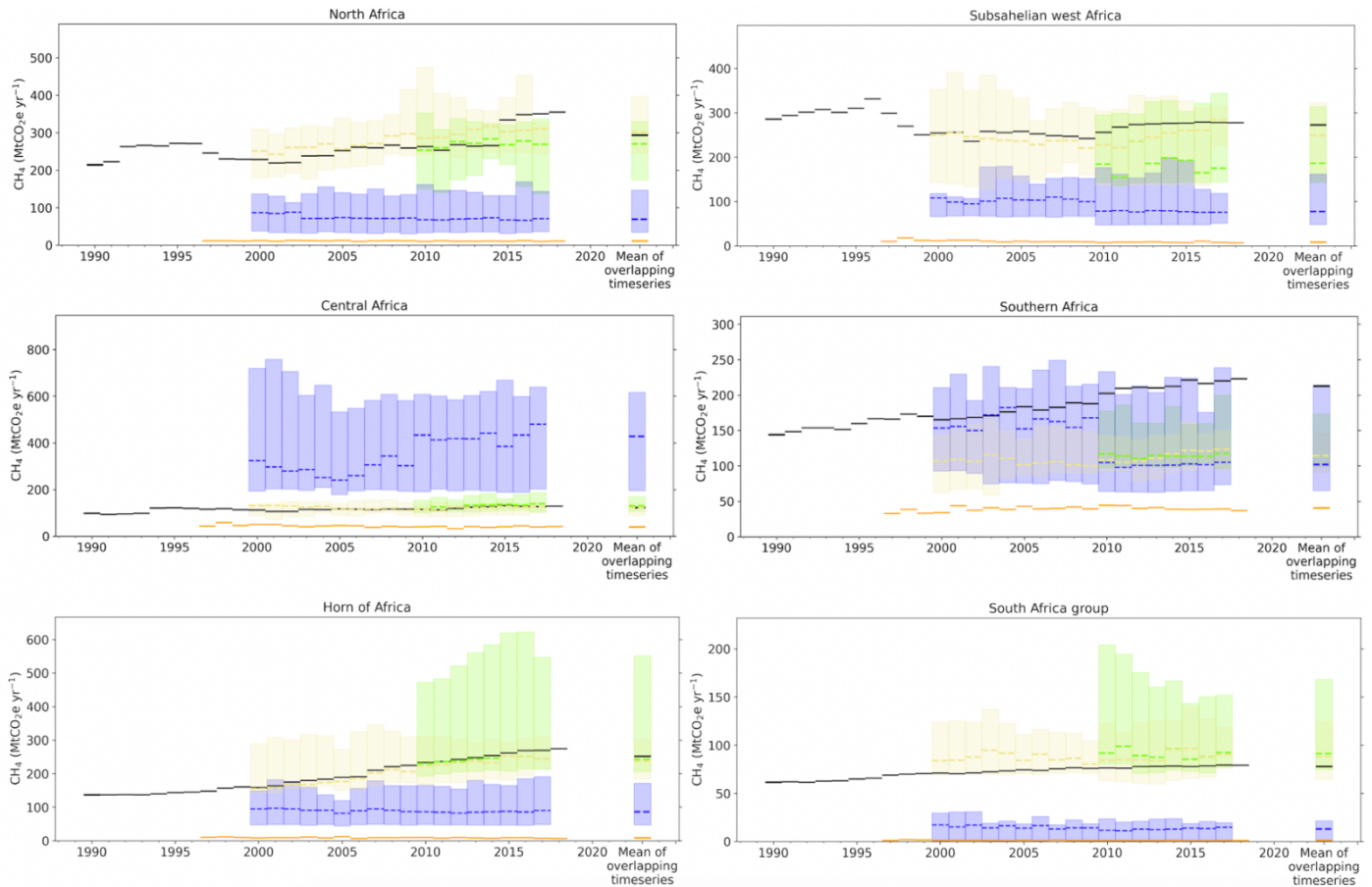
762
763 **Figure 7. Comparison of total anthropogenic CH$_4$ emissions in MtCO$_2$e yr^{-1} from the PRIMAP-hist inventory**
764 **(black) and global inversions. Shaded green and yellow areas represent the minimum and maximum range from**
765 **GOSAT satellite and surface inversions, respectively. Shaded blue areas represent the minimum and maximum**
766 **ranges of wetlands natural emissions from inversions. The orange lines represent wildfire emissions from GFED4.**
767

768 Figure 7 compares BU anthropogenic emissions from PRIMAP-hist for the period 2000-2018 with inversions'
769 anthropogenic emissions (see section 1). Wetlands natural emissions are shown in the figure only for
770 information from the median and range of inversions. Over the overlapping time period, medians of both
771 GOSAT and surface inversions are always smaller than PRIMAP-hist emissions, at continental and regional
772 level, except for the Central African region. For the African continent, the mean and min-max of GOSAT
773 inversions for anthropogenic CH$_4$ emissions over 2000-2018 is 1117^{1390}_{903} MtCO$_2$e yr^{-1}, very close to the mean
774 of surface inversions of 1094^{1330}_{853} MtCO$_2$e yr^{-1}. A good agreement between GOSAT and surface inversions
775 was also found in other high-emitting countries (Deng et al., 2021). In contrast, PRIMAP-hist gives a mean of
776 CH$_4$ anthropogenic emissions of 1231 MtCO$_2$e yr^{-1} over the period 2010-2017. The mean wetlands flux from
777 inversions over 2010-2017 is of 827^{946}_{481} MtCO$_2$e yr^{-1}. Methane emissions from wildfires over Africa for the
778 same period are less important, with a mean of 110 MtCO$_2$e yr^{-1}.

779   Regional emissions from PRIMAP-hist ranked in decreasing order are: North Africa (293 MtCO$_2$e yr^{-1}) > Sub-

780   Sahelian west Africa (272 MtCO$_2$e yr^{-1}) > Horn of Africa (252 MtCO$_2$e yr^{-1}) > Southern Africa (212 MtCO$_2$e

781   yr^{-1}) > Central Africa (123 MtCO$_2$e yr^{-1}) > South Africa (78 MtCO$_2$e yr^{-1}). For both GOSAT and surface

782   inversions, the ranking of regions (Table S11) is almost the same for surface inversions and PRIMAP-hist, with

783   the exception of Central Africa and Southern Africa.

784

785   **2.4 Results for N$_2$O emissions**

786   **N$_2$O PRIMAP-hist versus atmospheric inversions (total flux)**

787   **Total and sectoral N$_2$O anthropogenic emissions (PRIMAP-hist)**

788

789   **(a)**

798 **(b)**
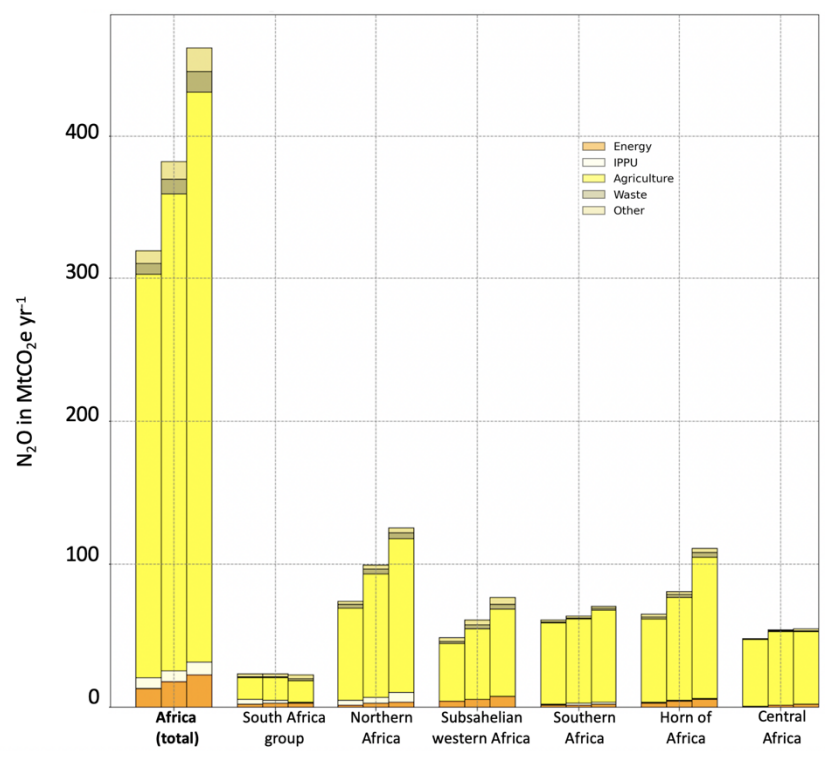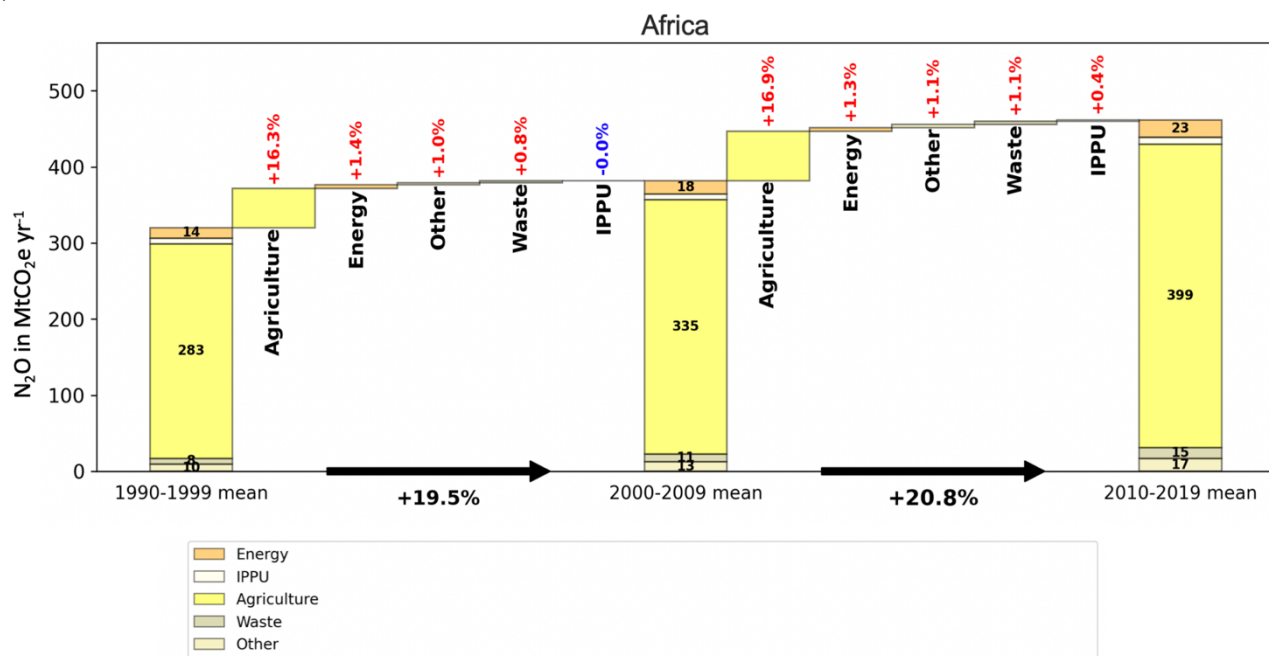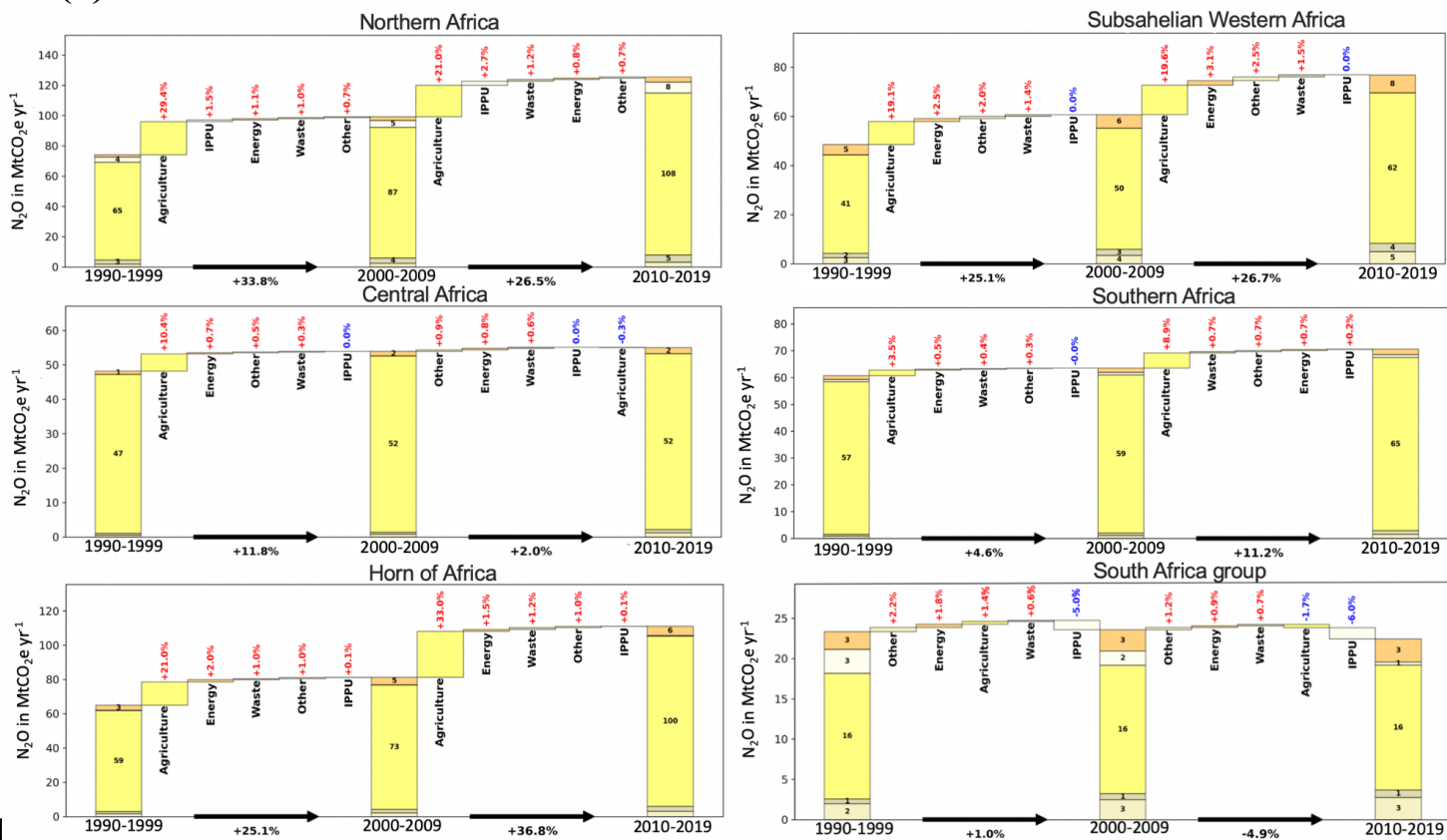
Figure 8. (a) African anthropogenic N_2O emissions in $MtCO_2e$ yr^{-1} over three decades: 1990-1998, 1999-2008 & 2009-2019. Data from PRIMAP-hist (2021). (b) Contribution of each sector to the change of African N_2O emissions between the last three decades. (c) Same for different regions regrouping several countries. Data from PRIMAP-hist (2021).

Figure 8 presents anthropogenic N_2O emissions from PRIMAP-hist, for five sectors (for country values, see Fig. 4). Over the last three decades, the mean African emissions are 378 $MtCO_2e$ yr^{-1}, three times less than CH_4 emissions. The mean decadal N_2O emissions increased from 319 $MtCO_2e$ yr^{-1} in 1990-1999, to 382 $MtCO_2e$ yr^{-1} in 2000-2009 (+20%), and further to 431 $MtCO_2e$ yr^{-1} in 2010-2018. Over the last three decades, the main emitting sector remained Agriculture. The N_2O emissions increase also originates from Agriculture, with an increase from 283 $MtCO_2e$ yr^{-1} to 335 $MtCO_2e$ yr^{-1} between 1990-1999 and 2000-2009, that is, +16.3 % compared to of the total emission increase of +19.5%. The three other sectors show a smaller contribution to the emissions increase: Energy (+1.4%), Other (+1%) and Waste (+0.8%). IPPU shows no change. Similarly, between 2000-2009 and 2010-2019, the N_2O emissions increase also came from the sector of Agriculture, with an increase from 335 $MtCO_2e$ yr^{-1} to 399 $MtCO_2e$ yr^{-1} between 1990-1999 and 2000-2009.

The main contributing regions to the continental emissions are Northern Africa and the Horn of Africa (Fig. 8a). Between 2000-2009 and 2010-2019, the North African contribution increased from 99 $MtCO_2e$ yr^{-1} to 125 $MtCO_2e$ yr^{-1} (+27%). The main sectoral contribution is always Agriculture, which increased in that region from 86 $MtCO_2e$ yr^{-1} to 107 $MtCO_2e$ yr^{-1} (+21%). Emissions from the second largest emitting region, the Horn of Africa, increased from 81.19 $MtCO_2e$ yr^{-1} in 2000-2009 to 111 $MtCO_2e$ yr^{-1} in 2010-2019 (+37%), mainly from Agriculture. In the third most emitting region, Sub-Sahelian Africa, emissions increased from 61 $MtCO_2e$ yr^{-1} in 2000-2009 to 77 $MtCO_2e$ yr^{-1} in 2010-2019 (+27%), also from Agriculture. The least contributing region to the increase of the total N_2O emissions from 2000-2009 to 2010-2019 is South Africa which had a very small decrease, mainly from IPPU (-6%) followed by Agriculture (-2%). On the contrary, there is a slight increase of N_2O emissions for the group of South Africa for the Other (+1%), Energy (+1%) and Waste (+1%) sectors.
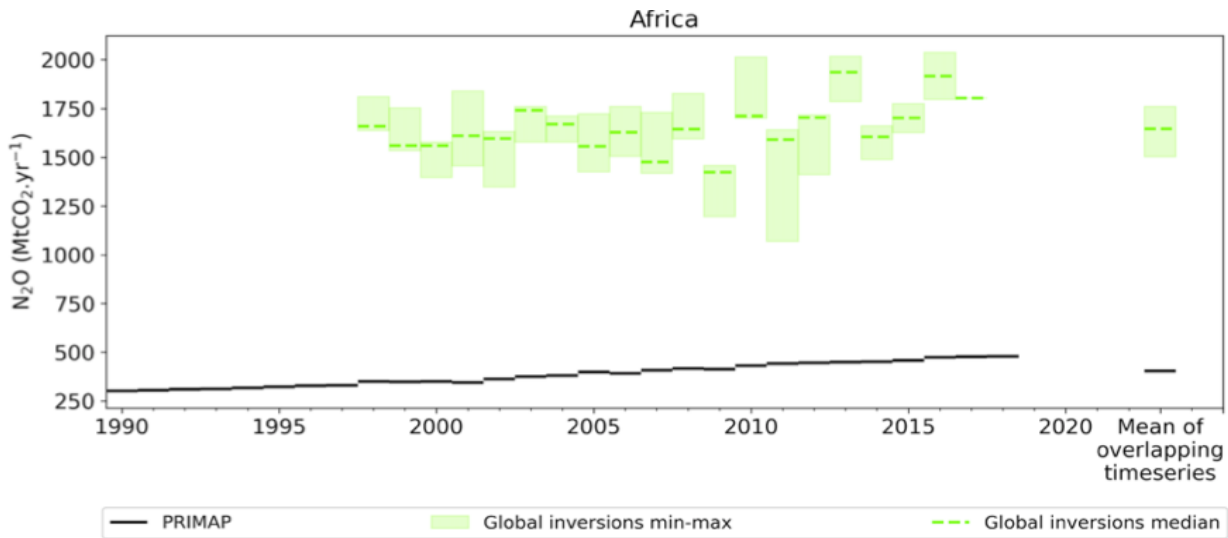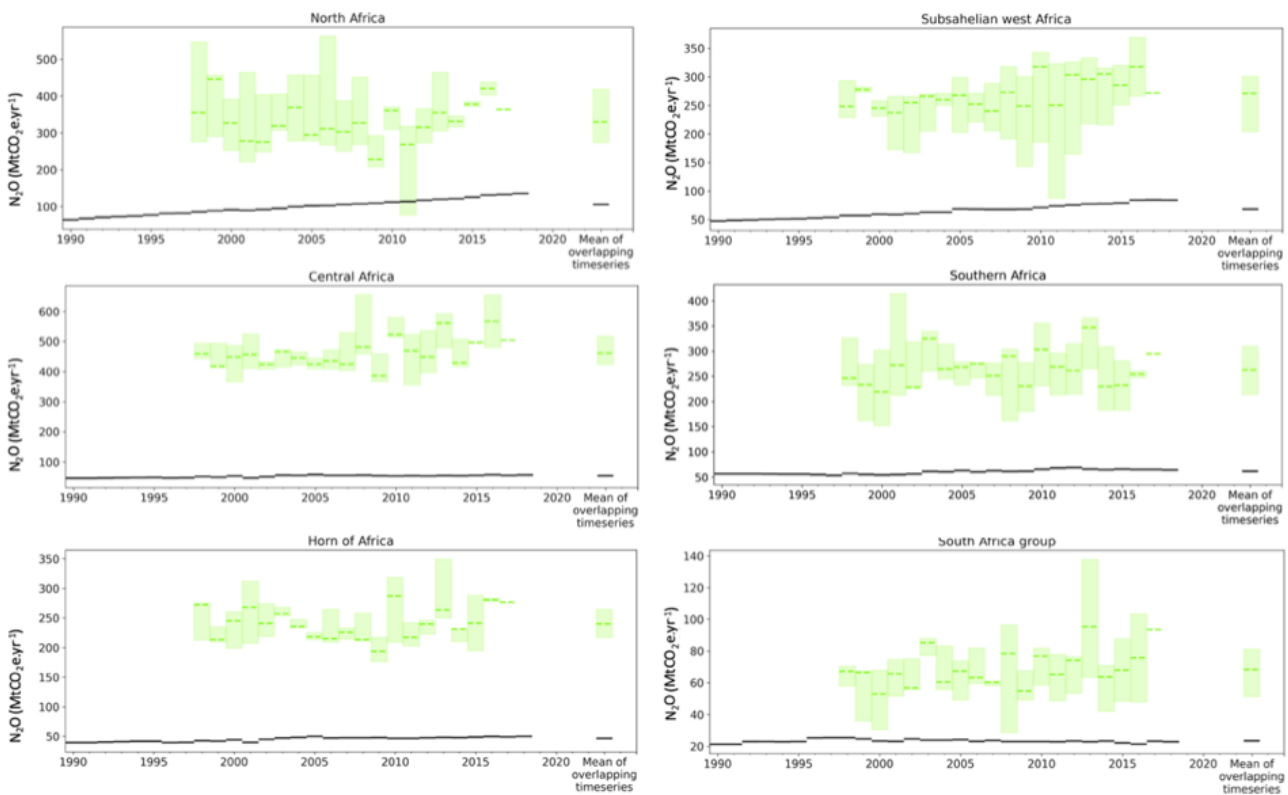
Figure 9. Total N₂O emissions from PRIMAP-hist in MtCO₂e yr⁻¹ (black line) from three GCP atmospheric inversions for the entire African continent and for six African sub-regions. The green line is the median of the three inversions and the light green areas the maximum-minimum range.

Figure 9 compares N_2O emissions from PRIMAP-hist and inversions. For total Africa, the mean of inversions emissions over the overlapping time period 1998-2017 is 1647^{1760}_{1502} MtCO₂e yr⁻¹, much larger than the PRIMAP-hist estimate of 360 MtCO₂e yr⁻¹. According to PRIMAP-hist, total African emissions increased by

834   28% between 1998 and 2017, while the trend of emissions from the inversions is $16 \pm 8\%$. At regional scale,

835   emissions from inversions ranked in decreasing order are: Central Africa (461_{424}^{517} MtCO₂e yr⁻¹ MtCO₂e yr⁻¹) >

836   North Africa (330_{274}^{419}MtCO₂e yr⁻¹) > Sub-Sahelian West Africa (271_{68}^{330}MtCO₂e yr⁻¹) > Southern Africa

837   (263_{214}^{310}MtCO₂e yr⁻¹ > Horn of Africa 240_{217}^{265} MtCO₂e yr⁻¹ > South Africa (68_{51}^{81}MtCO₂e yr⁻¹). According to

838   PRIMAP-hist, the ranking is: North Africa (106 MtCO₂e yr⁻¹) > Sub-Sahelian West Africa (68 MtCO₂e yr⁻¹) >

839   Southern Africa (62 MtCO₂e yr⁻¹) > Central Africa (54 MtCO₂e yr⁻¹) > the Horn of Africa (46 MtCO₂e yr⁻¹) >

840   South Africa (24 MtCO₂e yr⁻¹) (See also Table S13). Emissions from PRIMAP-hist are smaller than inversions

841   by a factor of 16. This is likely due to the fact that we did not attempt to separate natural from anthropogenic

842   emissions in inversions. Other studies (Ciais et al., 2021; Petrescu et al., 2021 in Europe) showed that even

843   after subtracting N₂O natural estimates, inversions always point to higher estimates than BU methods.

844

845   **3 Discussion: uncertainties, comparison between BU and TD methods, and synthesis for the three main**

846   **GHG**

847

848   **3.1 Uncertainties specific to DGVMs / inversions for LULUCF CO₂**

849

850   In Fig. 5, we showed important disagreements among models regarding LULUCF CO₂ on whether Africa has

851   been a small source over the last 20 years (as shown by inversions) or a net sink (as shown by DGVMs and

852   UNFCCC except with the Grassi et al. correction). There is also more interannual variability in the DGVMs

853   results, mainly from climate variability, which is absent from UNFCCC as inventories provide only decadal

854   smoothed flux estimates. The larger sink in the DGVMs compared to the corrected UNFCCC estimates using

855   the method of Grassi et al. (2022) may be due to the fact that non-Annex I UNFCCC estimates generally do

856   not include dead biomass or harvested wood products. If forest biomass is estimated by a stock-change

857   approach, therefore, changes in living biomass due to transfer to dead biomass and harvested wood products

858   will be considered emitted in that year, while in the DGVMs it will decay more slowly over time. Another

859   difference is the treatment of land use change emissions, based on historical global land use change maps for

860   the DGVMs, which can significantly differ from national land use datasets. On the other hand, DGVMs do not

861   represent forestry and may underestimate sinks in intensively managed young forests. DGVMs do not separate

862   between unmanaged and managed lands, while UNFCCC inventories only account for managed land, yet

863   including conservation areas and indigenous territories. Grassi et al. (2022) showed that the difference between

864   the global UNFCCC sink (1100 MtCO₂ yr-1) and the global land carbon sink (4767 MtCO₂e yr-1) must be

865   explained by the contribution of non-managed lands. But in the case of Africa, it was not possible to extract

866   from UNFCCC reports the national areas of unmanaged land, and we had to also look at UNFCCC Technical

867 Assessment Reports (TAR) as well as REDD+ reports to extract information. Methods of assessment have not
868 been fully standardized since 1990, and they differ depending on the countries analyzed, and on the emissions
869 categories considered. In this context, when comparing UNFCCC estimates with data from DGVM and
870 inversion models, different layers of aggregated uncertainties affect the analysis. (Deng et al., 2021; Petrescu
871 et al., 2021; Grassi et al., 2018). The fact that LULUCF CO_2 fluxes have the greatest uncertainties is true
872 globally.

873

874 **3.2 Differences and sources of uncertainties between BU and TD CH_4 emissions**

875

876 The methodology used for removing natural CH_4 emissions from inversions is key for comparing with BU
877 estimates of anthropogenic emissions only. In this paper, we used a separation based on the natural emissions
878 solved by each inversion (section 2.3 method 1). Using an alternative method from Deng et al. (2022) based on
879 natural emissions from the median of all inversions gives smaller anthropogenic emissions than PRIMAP-hist
880 (Fig. S10).

881

882 **3.3 Differences and sources of uncertainties between BU and TD N_2O emissions**

883

884 For N_2O emissions, discrepancies between inventories and inversions are very high, especially for the group of
885 Central African countries, where the vegetation covers an important land area with likely large natural N2O
886 (Deng et al., 2022). We can suppose that more broadly for all African groups, the lack of accounting of natural
887 emissions is the main reason why PRIMAP-hist estimates are much smaller than inversions. All African
888 countries used Tier 1 emission factors and include only direct N_2O emissions. The study by Deng et al. (2022)
889 underlined that indirect anthropogenic emissions notably coming from "atmospheric nitrogen deposition and
890 leaching from anthropogenic nitrogen additions to aquifers and inland water are usually not reported by non-
891 Annex I countries" and that this under-reported source of anthropogenic emissions tends to represent about 5%
892 to 10% of anthropogenic N_2O. According to Deng et al. (2022), the global situation from inversions for main
893 emitters is similarly affected by the potential contribution of natural sources as well, which is difficult to
894 estimate and separate. Figure 11 from Deng et al. (2022) shows that even when removing "intact / non-managed
895 lands" from inversions, in many countries, especially tropical countries, the inversions give a systematically
896 much higher anthropogenic level of N_2O than inventories, suggesting that there are either missing
897 anthropogenic sources or some "natural" sources (e.g. conservation areas) in managed lands being
898 underestimated by inventories.

899   **3.4 Synthesis of the steps for assessing net GHG trends over Africa**

900

901   Here, we propose a first step towards the elaboration of what could become a more systematic method for a

902   scientific benchmark of non-Annex I national inventories: 1) correct outliers, 2) check the plausibility of

903   estimates, 3) have an independent evaluation of inventory data by experts, 4) a comparison between UNFCCC

904   data corrected thanks to expert judgment and other BU and TD methods, 5) computation of the mean of all

905   BU and TD methods, 6) computation of "best fitted BU values" (meaning "best fitted BU values" excluding

906   uncorrected UNFCCC data), and "TD values" (meaning "best fitted TD values": without considering N_2O

907   inversions replaced with PRIMAP-hist values), 7) identification of ranking anomalies.

908

909   **3.5 Net GHG budget from inversions**
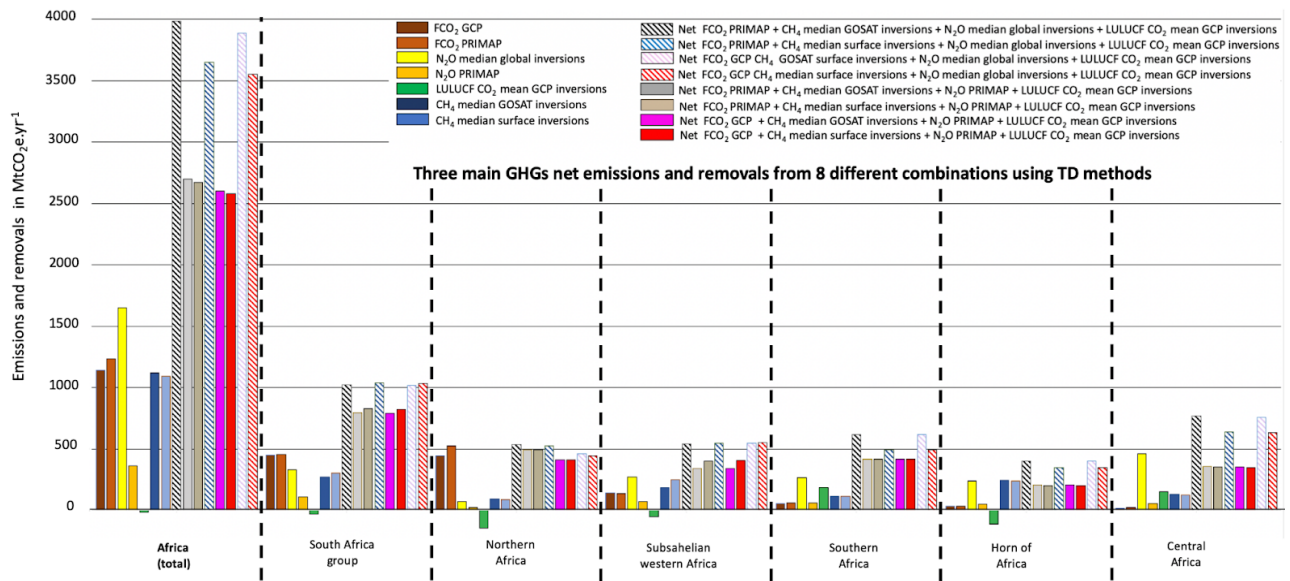
910
911   **Figure 10. Synthesis for the three main GHG with net African budget computation by all TD methods for Africa**

912   **as a whole and for six sub-groups of African countries across overlapping time series (2001-2017). Following the**

913   **atmospheric convention, positive numbers represent an emission to the atmosphere and the negative values**

914   **represent a sink. The CO₂ emissions and sinks from LULUCF are represented in green, they are taken from GCP**

915   **2020 dataset. Unit is MtCO₂e yr⁻¹.**

916

917   Figure 10 shows different combinations of inversion GHG budgets and individual gasses contributions.

918   For total Africa, the mean net GHG budget from inversions where N_2O inversions are replaced by PRIMAP-

919   hist is 2638^{5873}_{1761} MtCO₂e yr⁻¹. Regional GHG budgets in decreasing order are: North Africa $(810^{1170}_{279}$

920   MtCO₂e yr⁻¹) > South Africa group $(452^{751}_{161}$ MtCO₂e yr⁻¹) > Southern Africa $(416^{1465}_{-334}$ MtCO₂e yr⁻¹) > Sub-

921   Sahelian West Africa $(373^{1051}_{36}$MtCO₂e yr⁻¹) > Central Africa $(352^{1592}_{-1133}$ MtCO₂e yr⁻¹) > Horn of Africa

922     $(204^{873}_{456}$ MtCO$_2$e yr^{-1}) (Table S17). The mean net of inversions including N$_2$O inversions is substantially

923   higher, 3879^{7341}_{1320} MtCO$_2$e yr^{-1}. Regional GHG budgets in decreasing order are: North Africa

924     $(1034^{1475}_{600}$ MtCO$_2$e yr^{-1}) > Central Africa $(759^{2054}_{-763}$ MtCO$_2$e yr^{-1}) > Southern Africa $(616^{1713}_{-262}$ MtCO$_2$e yr^{-1}) >

925   Sub-Sahelian West Africa $(576^{1313}_{-61}$ MtCO$_2$e yr^{-1}) > South Africa group $(496^{814}_{138}$ MtCO$_2$e yr^{-1}) (Table S17).

926

927   **3.6 Comparison between BU and TD methods**
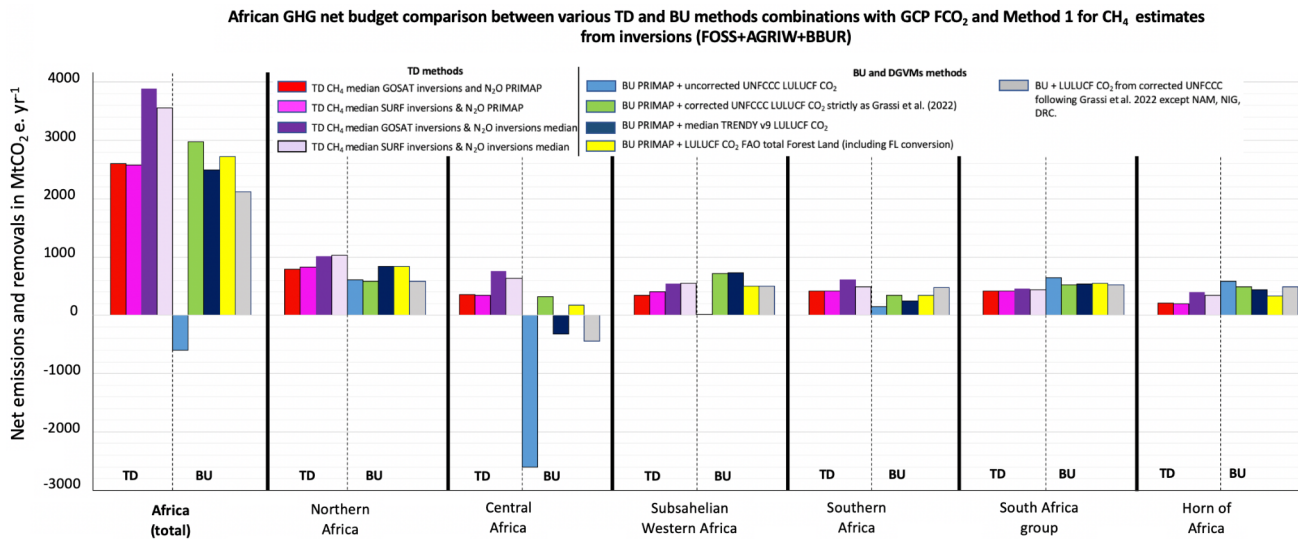
928
929
930 **Figure 11. Synthesis for the three main GHG net African budget from TD and BU methods, using Method 1 for**

931 **separating anthropogenic CH$_4$ emissions from inversions (FOSS+AGRIW+BBUR) during 2001-2017. FCO$_2$ data**

932 **from GCP. N$_2$O from global inversions and from PRIMAP-hist. For TD methods, anthropogenic CH$_4$ from both**

933 **GOSAT and surface inversions are used, and LULUCF from GCP inversions only. For BU methods, anthropogenic**

934 **CH$_4$ and N$_2$O from PRIMAP are used, and with five different methods for assessing LULUCF CO$_2$: from**

935 **uncorrected UNFCCC data; from corrected UNFCCC data according Grassi et al. (2022); from corrected**

936 **UNFCCC except Namibia, Nigeria and DRC; from TRENDY v9; from FAO FL including FL conversions.**

937 **Following the atmospheric convention, positive numbers represent an emission to the atmosphere and the negative**

938 **values represent a sink. All values are in MtCO$_2$e.**

939
940 Figure 11 shows the GHG budgets from all combinations of BU and TD methods. The mean of all methods

941 after filtering outliers (Grassi et al. (2022) UNFCCC corrections, using PRIMAP instead of inversions for N$_2$O)

942 is 2630^{4557}_{1974} MtCO$_2$e yr^{-1}, which represents only 7.3 % of global FCO$_2$ emissions. The mean of all estimates

943 points out to a source in the six African regions ranked in decreasing order as: North Africa $(761^{988}_{460}$ MtCO$_2$e

944 yr^{-1} $(513^{702}_{161}$ MtCO$_2$e yr^{-1}) > Horn of Africa $(318^{699}_{-80}$ MtCO$_2$e yr^{-1}) > Sub-Sahelian West Africa

945 $(492^{913}_{286}$ MtCO$_2$e yr^{-1}) > Southern Africa $(354^{998}_{-78}$ MtCO$_2$e yr^{-1}) > Central Africa $(143^{882}_{-670}$ MtCO$_2$e yr^{-1}).

946   We initially did not make any assumption regarding which approach is "better" between TD and BU method,
947   as it actually depends on the considered gas, sector and spatial scale. Comparability between TD and BU results
948   is not completely obvious either, as they do not represent the same processes (example of LULUCF CO_2 for
949   DGVM as explained in paragraph 3.1). For N_2O specifically, we highlighted in paragraph 3.3 the large
950   uncertainty of the TD estimates, underlining the importance to separate natural N_2O emissions from total
951   estimates in order to deliver appropriate anthropogenic assessments thanks to the inversions.
952

953   We showed in the results of this paper that inversions in general tend to have larger uncertainties than
954   inventories, and large differences in terms of min / max and at annual scale even among similar typologies of
955   the methods. But at a decadal scale, they deliver reliable overall trends (with good match among the median
956   values of various estimates on the overlapping time period) especially at the spatial scale of groups of countries
957   and of a continent. Under such conditions, TD estimates help identify or confirm outliers / large uncertainties
958   in inventories that may occur especially for Non-annex I countries like Africa.
959

960   Inversions therefore can't be a substitute but rather a complement to check trends consistency of inventories
961   and help to identify and correct main outliers. That's why we chose BU estimates to deliver a final budget over
962   Africa (with CO_2 LULUCF corrections) as synthesis figures (see Fig.12 and Fig.13 in the next paragraph).
963   Possibilities to reduce the gap BU and TD estimates are the following: 1) For inversions: to have a coarser
964   network of surface stations and coarser spatial resolution. 2) For DGVM: see paragraph 3.1. 3) For national
965   UNFCCC inventories: to have regularly updated activity data and use country-specific emissions data and
966   include indirect emissions, which is not the case to date for African countries, and use expert judgment for
967   correcting outliers as done by Grassi et al. (2022) and in this study for CO_2 LULUCF emissions.

3.7 Net GHG budget from BU estimates

969
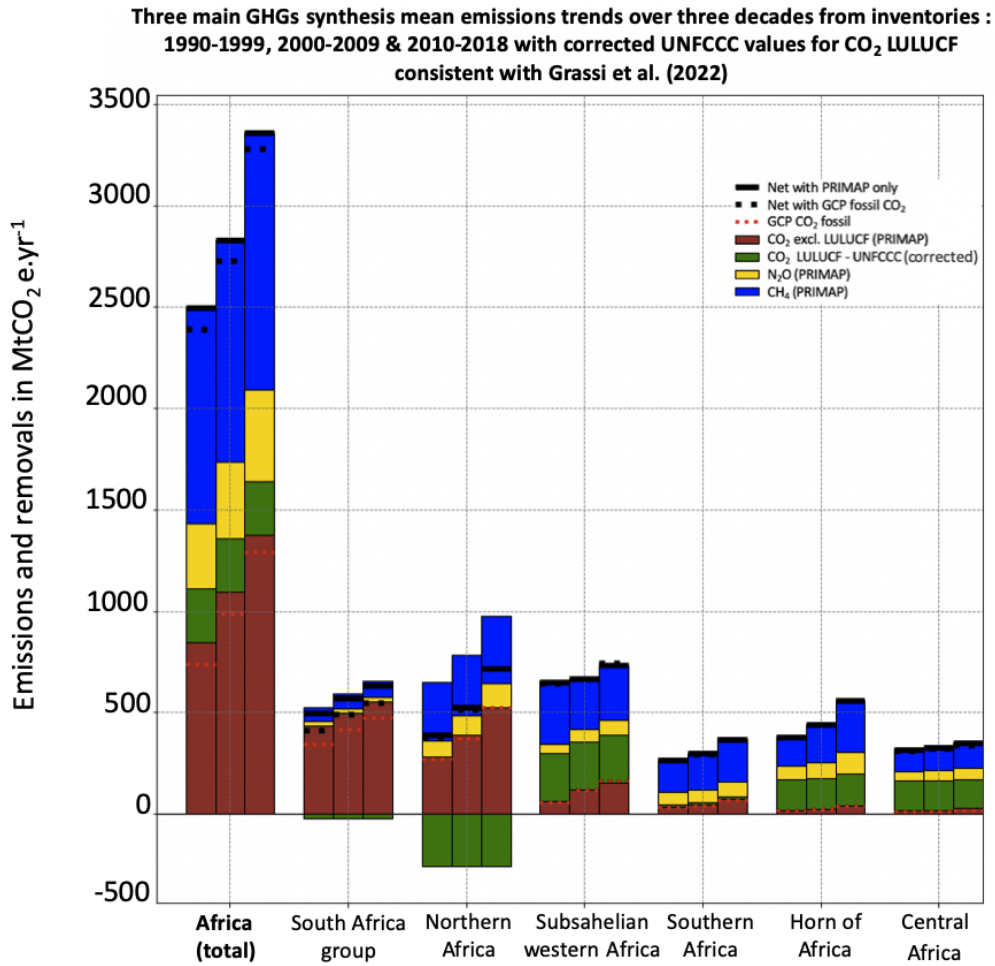
Figure 12. Synthesis for the three main GHG from inventories (after UNFCCC LULUCF CO₂ corrections
consistent with Grassi et al. (2022)) for the three main GHG with net African budget computation by BU inventories
for Africa as a whole and for six sub-groups of African countries across three different decades (1990-1999, 2000-
2010, 2010-2018) using data and corrections from country inventories. Following the atmospheric convention,
positive numbers represent an emission to the atmosphere and the negative values represent a sink. Black
horizontal lines represent a net flux resulting from the addition of the three main GHG using PRIMAP-hist only,
dashed black horizontal lines also represent the net flux resulting from the addition of the three main GHG but
using the GCP dataset for FCO₂. Dashed red lines represent the fluxes from GCP FCO₂ available in the most recent
GCP paper, to compare them with PRIMAP-hist results which are represented with the brown bar plots. The N₂O
and CH₄ fluxes from PRIMAP-hist are respectively represented with yellow and blue bars. CO₂ emissions and
sinks from LULUCF are represented in green, they are taken from NC/BUR UNFCCC datasets with corrections
applied. Unit is MtCO₂e yr⁻¹.

Figure 12 shows the budget for the three GHG from UNFCCC data with LULUCF data corrected using the second approach. There is a clear increase of African total GHG emissions during the last 3 decades. The differences between BU datasets are mainly due to different sectoral allocations. However, the trends are consistent and comparable, and differences among inventories tend to be less for the most recent decade.

Table 5. Mean net total Africa and regional groups' emissions and removals from BU methods using either GCP or PRIMAP-hist for FCO_2 over 2001-2017 in $MtCO_2e.yr^{-1}$.

	Type of dataset									
	BU methods with GCP FCO_2						BU methods with PRIMAP FCO_2			
Region	GCP + uncorrected UNFCCC LULUCF CO_2	GCP + corrected UNFCCC LULUCF CO_2 as Grassi et al. (2022)	GCP + corrected UNFCCC LULUCF CO_2 as Grassi et al. (2022) but for DRC, NAM, NIG	GCP + median TRENDY v9 LULUCF CO_2 (min/max)	GCP + LULUCF CO_2 FAO total FL		PRIMAP + uncorrected UNFCCC LULUCF CO_2	PRIMAP + corrected UNFCCC LULUCF CO_2 as Grassi et al. (2022)	PRIMAP + corrected UNFCCC LULUCF CO_2 as Grassi et al. (2022) but for DRC, NAM, NIG	PRIMAP + median TRENDY v9 LULUCF CO_2 (min/max)	PRIMAP + LULUCF CO_2 FAO total FL
Africa total	-599	2975	2122	2478_{732}^{4806}	2728		-502	3069	2216	2572_{827}^{4899}	2822
North Africa	613	589	589	835_{549}^{1216}	839		620	597	597	842_{557}^{1224}	846
Central Africa	-2605	316	-448	-318_{-879}^{633}	171		-2598	324	-440	-310_{-871}^{641}	179
Subsahelian West Africa	19	718	501	726_{433}^{1382}	503		15	714	497	723_{430}^{1378}	500
Southern Africa	149	346	473	251_{-453}^{953}	345		151	347	475	252_{-452}^{955}	346
South Africa group	640	524	524	542_{179}^{860}	546		719	603	603	621_{258}^{939}	625
Horn of Africa	586	484	484	438_{-109}^{805}	325		587	484	484	439_{-108}^{806}	326

At the country level, a small number of countries showed an increasing difference between PRIMAP-hist and GCP estimates of fossil CO_2 emissions over time, but they are small FCO_2 emitters. The differences may also be partly explained by changes in accounting methods as mentioned in Gütschow et al. (2016). The biggest discrepancies are noticeable for Mali (64%), Cameroon (-62%), and the DRC (-38%), but those three countries are not major FCO_2 emitters (Fig. 4.a-b).

Table 5 shows the differences of net African budget from various BU methods using GCP or PRIMAP-hist for FCO_2 over 2001-2017 that are also illustrated on Fig. 11.

BU LULUCF budget from UNFCCC corrected by Grassi (2022)

Over 2001-2017 the net BU GHG budget is 2975 MtCO$_2$e yr^{-1}. Regionally the ranking in decreasing order is: Sub-Sahelian West Africa (718 MtCO$_2$e yr^{-1}) > North Africa (588 MtCO$_2$e yr^{-1}) > South Africa group (524 MtCO$_2$e yr^{-1}) > Horn of Africa (484 MtCO$_2$e yr^{-1}) > Southern Africa (346 MtCO$_2$e yr^{-1}) > Central Africa (316 MtCO$_2$e yr^{-1}).

BU LULUCF budget CO$_2$ from FAO

The BU budget from FAO data is 2728 MtCO$_2$e yr^{-1}, 8% less than above. The ranking of regions in decreasing order is: North Africa (838 MtCO$_2$e yr^{-1}) > South Africa group (546 MtCO$_2$e yr^{-1}) > Sub-Sahelian West Africa (503 MtCO$_2$e yr^{-1}) > Southern Africa (345 MtCO$_2$e yr^{-1}) > Horn of Africa (325 MtCO$_2$e yr^{-1}) > Central Africa (171 MtCO$_2$e yr^{-1}).

BU LULUCF budget from DGVMs

The net GHG budget for Africa is 2478^{4806}_{733} MtCO$_2$e yr^{-1}, 9% less than with FAO. The ranking of regions in decreasing order is: North Africa (835^{1216}_{549} MtCO$_2$e yr^{-1}) > Sub-Sahelian West Africa (726^{1382}_{433} MtCO$_2$e yr^{-1}) > South Africa (542^{859}_{179} MtCO$_2$e yr^{-1}) > Horn of Africa (438^{805}_{-109} MtCO$_2$e yr^{-1}) > Southern Africa (251^{953}_{-453} MtCO$_2$e yr^{-1} > Central Africa (-318^{633}_{-879} MtCO$_2$e yr^{-1}).
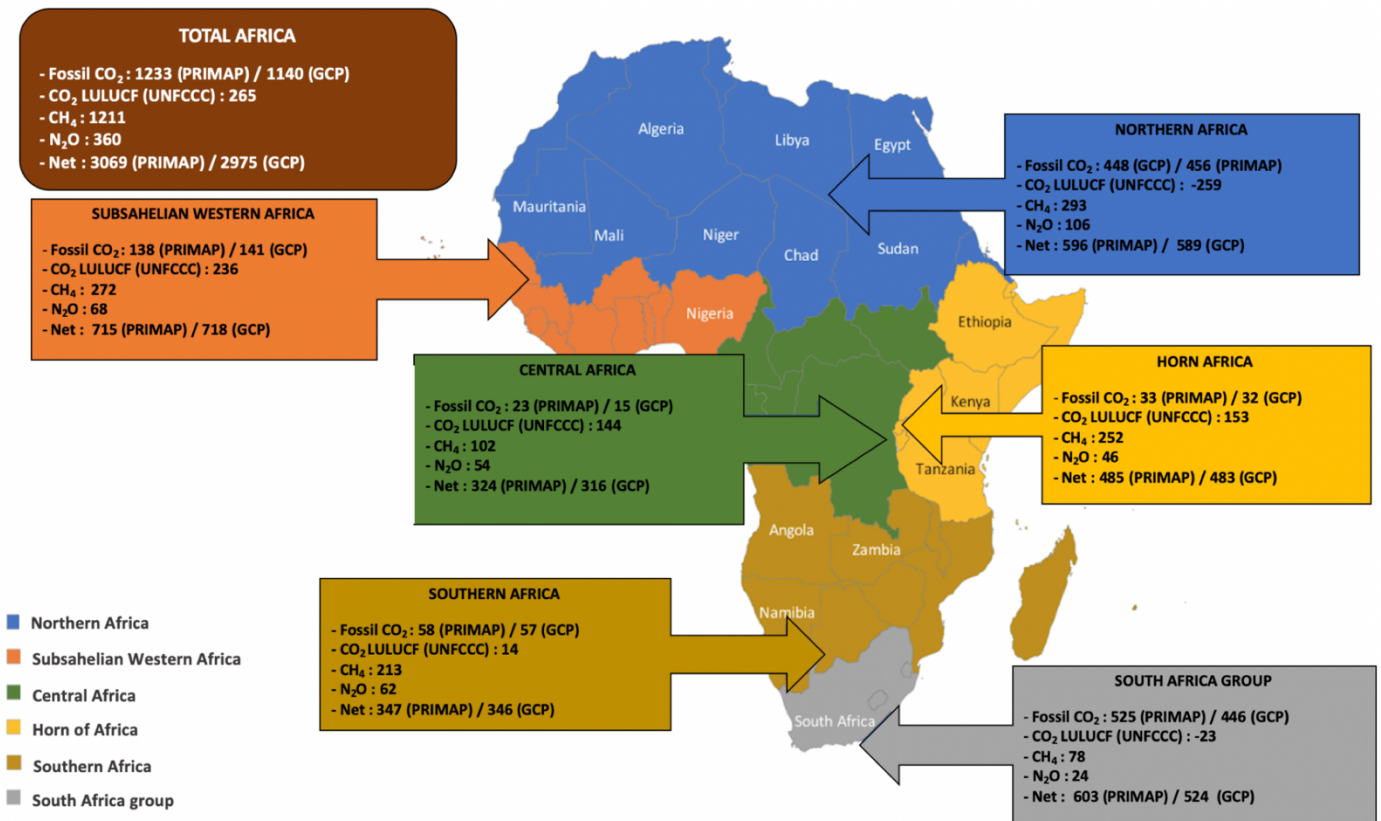
Figure 13. 2001-2018 emissions in MtCO₂e yr⁻¹ for fossil CO₂ (GCP and PRIMAP-hist), LULUCF CO₂ (corrected UNFCCC data consistent with Grassi et al. (2022), CH₄ (PRIMAP-hist), N₂O (PRIMAP-hist) for Africa, and for six regions.

For information, in the supplement section Fig. S13 and Fig. S14 illustrate the differences in MtCO₂e and in % for CH₄, N₂O and for the total net GHG budget that would result from the use of AR6 GWP100 compared to AR4 GWP100 currently in used by UNFCCC non-Annex I countries, for the six African regions considered on Fig.13 as well as for Africa total. The net difference on the total African budget for the use of GWP100 AR6 instead of AR4 is: +4.6%, which means a relatively small increasing impact on the net budget, with a prevailing effect of the slight increase of CH₄ GWP100 in the AR6 as compared to AR4, over the strong decrease of N₂O GWP-100. The two African regions that are the most impacted in terms of net budget are: Southern Countries (+7.2%) and the Horn of Africa (+6.3%). The least impacted region in terms of overall net budget with an updated AR6 GWP-100 for CH₄ and N₂Ois South Africa (+1.7%).

4 Summary, concluding remarks and perspectives

Africa is a large continent gathering 56 countries, and some countries are major GHG emitters. Because of its rapidly growing population and high industrial potential, Africa is a critical geography regarding climate change mitigation and adaptation policy. Depending on the emissions pathways, Africa, which is already a big emitting region, is expected to represent between at least a bit more than 10% of the global share by 2050, and could become as high as 18% of global emissions by 2050 (van der Zwaan, 2018).

This paper delivers both a continental view and a detailed analysis of the three main GHG trends during the last thirty years across this continent as a whole, across relevant groups of countries given the inversions' resolutions, and also considering country details. Thanks to the comparison of different methods and datasets, the uncertainty about the net emissions and removals of GHG lowers. The interest of studying Africa is high not only from a scientific point of view, but also from a climate-policy perspective, as under the UNFCCC principle of "common but differentiated responsibility" about global warming, the credibility of the PA lies in the effective participation and inclusiveness of all parties, including non-Annex I countries. Our effort of comparing BU datasets and inversions and analyzing differences for African GHG emissions and removals assessment by looking at trends since 1990 will also be useful for future updates on a regular basis within the 2023 GST perspective.

At the scale of Africa, there is a rapid increase of FCO₂ emissions that roughly doubled since 1990. This increase is dominated by coal emissions for the decade 1990-1998 compared to 1999-2008 (+9%), and by oil for the

decade 1999-2008 compared to the decade 2008-2017 (+16%). As for CO_2 LULUCF, we found that BU estimates are featured with important annual fluctuations, as opposed to periodic national inventories assessments, the reconciliation between the sectoral classification for anthropogenic estimates between TD and BU has to be done "manually" and is not uniform to date, which doesn't facilitate the comparability of those different approaches. There are also differences among GCP inversions for CO_2, due to the fact that choices of model transport may differ among models, because prior fluxes can also differ between modeling teams, and because the African GHG observation network is featured with few stations and relatively scarce data. The lack of integration of CO_2 lateral anthropogenic and river fluxes is also an issue to be taken into account when trying to compare BU and TD methods (Ciais et al., 2022), and in the present study we did integrate those lateral fluxes. Anthropogenic CH_4 from PRIMAP-hist estimates indicate that out of the total African emissions increase from 1064 $MtCO_2e$ yr^{-1} to 1116 $MtCO_2e$ yr^{-1} between 1990-2000 and 2001-2009 (+5%), only two sectors contributed: Agriculture, in a dominant way (+8%) and Waste (+5%). Energy contributes to emissions decrease (-8%) that is however too small to offset other sectors' CH_4 emissions that represent a net increase. The main regional contributions come from North Africa and from the Agriculture sector (+12%). Over the same period, the least contributing emitter is the group of South Africa (+12%), with only one decreasing emissions sector: Agriculture (-1%). The mean 2001-2009 emissions increased by +15% over 2010-2018 with contribution from all sectors except IPPU. This increase is dominated by Agriculture (+8%) and Waste (+ 6%). For 2010-2018, the two main contributing regions for CH_4 emissions are Northern Africa and Sub-Sahelian Western Africa, Agriculture being the dominant emitting sector. From inversions, after withdrawing natural emissions and wildfires using the GFED dataset from total CH_4 emissions, median values are almost always below PRIMAP-hist estimates. CH_4 natural emissions have an important impact in Africa especially in the Central African region as well as in the Southern countries. N_2O TD estimates are always higher than the ones from PRIMAP-hist, underlining the importance to separate natural N_2O emissions from total estimates in order to deliver appropriate anthropogenic assessments thanks to the inversions.

To compute a net budget for the three main GHG emissions and removals and for comparability we used the $MtCO_2e$ yr^{-1} metric and the latest IPCC report recommended GWP. The choice of a constructed GWP metric, however, creates additional associated uncertainties notably due to the selected time horizon. By computing the mean of methods excluding uncorrected UNFCCC and N_2O inversions data from twenty different ways for assessing GHG emissions and removals in Africa, we found that the most recent net from the three main GHG in Africa is a source of 2630^{4557}_{1974} $MtCO_2e$ yr^{-1}.

Our assessment of African GHG emissions trends over 30 years through different methods can enable comparisons of *ex post* with *ex ante* pledges of the PA, whose baseline year is often 1990. However, given the global geopolitics to date featured with the prevailing principle of national sovereignty, a scientific assessment

1079   of GHG can only work as a supporting tool (Janssens-Maenhout et al., 2020) and cannot be directly policy-

1080   prescriptive. We note a relatively good match among the various types of estimates in terms of overall trends,

1081   especially at a regional level and on a decadal basis, but large differences in terms of min / max and at annual

1082   scale even among similar typologies of the methods (TD or BU). The large discrepancies are a scientific limit

1083   to the possibility of precise verification of the African country-reported emissions, but they are good enough

1084   to indicate trends. To compute a net from the three main GHG, no purely "TD" method is available due to the

1085   necessity to replace N_2O inversions data with BU data. An original result of this study is that we proposed at a

1086   small scale what may become a systematic formalized methodological protocol for independent verification of

1087   a net estimate using country-reported data, to be possibly implemented at the UNFCCC secretariat scale in a

1088   centralized way. The African GHG increasing trend is not in line with the mitigation aims of the PA towards

1089   net-zero globally. Research teams focusing on inversion methods (Nickless et al., 2020), underline that

1090   uncertainties should not be above 15% in order to deliver a reasonable verification support capacity. A major

1091   source of complexity for the evaluation of the respect of the Paris Agreement comes from the fact that national

1092   pledges generally fall below the discrepancies between different scientific independent estimates. This calls for

1093   investments not only in improvements of atmospheric measurement devices but also in the research efforts for

1094   standardizing verification methods. At the policy level, the extrapolation of this study to the climate policy

1095   field could also serve as a compelling argument for the creation of a global dedicated "Climate Inspection task

1096   force" of the UNFCCC.

1097   **5 Data availability**

1098   The datasets from the three main greenhouse gasses used in this paper (CO_2, CH_4, N_2O) from the various BU

1099   inventories, TD inversions and DGVM over Africa will be made publicly available. This database is available

1100   from Zenodo at: https://doi.org/10.5281/zenodo.7347077 (Mostefaoui et al., 2022).

1101   This dataset contains 32 data files:

1102   **- CO_2 inversions** (annual flux for LULUCF CO_2)

1103   - African CO_2 TD inversions GCB2020 1990-2019: annual CO_2 flux from GCB inversion models

1104   - African CO_2 lateral flux 2001-2019: annual CO_2 lateral flux including river transport, crop and wood

1105   product trade.

1106   - African CO_2 TRENDYv9 1990-2019: annual CO_2 flux from 14 DGVM

1107   - FAO 1990-2019: annual emissions and removals from FAO dataset

1108   - Inventory IPCC 1990-2019: annual flux from inventory data collected from UNFCCC national

1109   inventories in the IPCC categories

1110   **- CH_4 inversions 2000-2017** (annual flux)

1111   - African CH_4 global inversion 2000-2017: CH_4 flux over 2000-2017 from 11 surface inversion and 11

1112 satellite inversion models from four sectors; fossil refers to emissions from the fossil sector; agriculture and

1113 waste refers to emissions from both the agriculture and waste sector; biomass burning refers to emissions from

1114 biomass burning

1115   - GFEDv4 1997-2016: wildfire emissions from the Global Fires Emission Dataset (GFED) version 4

1116 **- N_2O inversions 1998-2017** (annual flux)

1117   - N_2O PYVAR 1998-2017: total N_2O emissions from PyVAR inversions;

1118   - N_2O TOMCAT-INVICAT 1998-2015: total N_2O emissions from TOMCAT-INVICAT model;

1119   - N_2O MIROC4 - ACTM 1998-2016: total N_2O emissions from MIROC4-ACTM model;

1120 Data used in this study are also included in the Supplementary Information (for example, from FAO data) and

1121 on public websites (CDIAC, PRIMAP-hist, World Bank data). Any other data that support the findings of this

1122 study are available from the corresponding author upon request.

1123

1124 **Author contributions.** MM, PC, PP and MJM designed research and led the discussions; MM wrote the initial

1125 draft of the paper and edited all the following versions; MM made all figures ; MJM and PP processed the

1126 original data from inversions and DGVM; MM processed the UNFCCC data and corrections; PC, PP and YE

1127 gave valuable suggestions to the manuscript structure; PC, MJM and PPP read, gave comments and advice on

1128 previous versions of the manuscript; all co-authors commented on specific parts related to their datasets; PC,

1129 MJM, PP, FC, SS, CR, IL, MS, PP are data providers.

1130 **Competing interests.** The authors declare that they have no conflict of interest.

1131

1132 **Disclaimer.** The views expressed in this publication are those of the authors.

1133

1134 **Acknowledgements**

1135 MM acknowledges funding from Sorbonne University, Institute of the Environmental Transition. PC, PP, and

1136 MJM were supported by the European Commission, Horizon 2020 Framework Program (VERIFY, grant no.

1137 776810). PC and YE are also supported by the RECCAP2 project (grant no. ESRIN/4000123002/18/I-NB).

1138 We acknowledge Stephen Sitch and Trendy modelers for the use of their dataset. We also acknowledge

1139 Christian Rödenbeck for the use of CarboScope, Frédéric Chevallier for CAMS, Ingrid Luijkx for CTE,

1140 Marielle Saunois for CH_4 inversions. The PyVAR-N_2O modeling results were provided by Rona Thompson

1141 (NILU) and were funded through the Copernicus Atmosphere Monitoring Service

1142 (https://atmosphere.copernicus.eu/), implemented by ECMWF on behalf of the European Commission, and

1143 were generated using computing resources from LSCE.

References

Andrew, R. M.: A comparison of estimates of global carbon dioxide emissions from fossil carbon sources, Earth Syst. Sci. Data, 12, 1437–1465, https://doi.org/10.5194/essd-12-1437-2020, 2020.

Ayompe, L. M., Davis, S. J., and Egoh, B. N.: Trends and drivers of African fossil fuel CO_2 emissions 1990–2017, Environ. Res. Lett., 15, 124039, https://doi.org/10.1088/1748-9326/abc64f, 2020.

BP. BP Statistical Review of World Energy, 2020.

Beck, H. E., Zimmermann, N. E., McVicar, T. R., Vergopolan, N., Berg, A., and Wood, E. F.: Present and future Köppen-Geiger climate classification maps at 1-km resolution, Sci. Data, 5, 180214, https://doi.org/10.1038/sdata.2018.214, 2018.

Bombelli, A., Henry, M., Castaldi, S., Adu-Bredu, S., Arneth, A., de Grandcourt, A., Grieco, E., Kutsch, W. L., Lehsten, V., Rasile, A., Reichstein, M., Tansey, K., Weber, U., and Valentini, R.: An outlook on the Sub-Saharan Africa carbon balance, Biogeosciences, 6, 2193–2205, https://doi.org/10.5194/bg-6-2193-2009, 2009.

Canadell, J. G., Raupach, M. R., and Houghton, R. A.: Anthropogenic CO2 emissions inAfrica, Biogeosciences, 6, 463–468, https://doi.org/10.5194/bg-6-463-2009, 2009.

Chevallier, F., Fisher, M., Peylin, P., Serrar, S., Bousquet, P., Bréon, F.-M., Chédin, A., and Ciais, P.: Inferring CO2 sources and sinks from satellite observations: Method and application to TOVS data, J. Geophys. Res. Atmospheres, 110, https://doi.org/10.1029/2005JD006390, 2005.

Ciais, P., Bastos, A., Chevallier, F., Lauerwald, R., Poulter, B., Canadell, J. G., Hugelius, G., Jackson, R. B., Jain, A., Jones, M., Kondo, M., Luijkx, I. T., Patra, P. K., Peters, W., Pongratz, J., Petrescu, A. M. R., Piao, S., Qiu, C., Von Randow, C., Regnier, P., Saunois, M., Scholes, R., Shvidenko, A., Tian, H., Yang, H., Wang, X., and Zheng, B.: Definitions and methods to estimate regional land carbon fluxes for the second phase of the REgional Carbon Cycle Assessment and Processes Project (RECCAP-2), Geosci. Model Dev., 15, 1289–1316, https://doi.org/10.5194/gmd-15-1289-2022, 2022.

Deng, Z., Ciais, P., Tzompa-Sosa, Z. A., Saunois, M., Qiu, C., Tan, C., Sun, T., Ke, P., Cui, Y., Tanaka, K., Lin, X., Thompson, R. L., Tian, H., Yao, Y., Huang, Y., Lauerwald, R., Jain, A. K., Xu, X., Bastos, A., Sitch, S., Palmer, P. I., Lauvaux, T., d'Aspremont, A., Giron, C., Benoit, A., Poulter, B., Chang, J., Petrescu, A. M. R., Davis, S. J., Liu, Z., Grassi, G., Albergel, C., and Chevallier, F.: Comparing national greenhouse gas budgets reported in UNFCCC inventories against atmospheric inversions, Earth Syst. Sci. Data Discuss., 1–59, https://doi.org/10.5194/essd-2021-235, 2021.

Dorfman, R.: A formula for the Gini Coefficient. The Review of Economics and Statistics Vol. 61, No. 1 , https://doi.org/10.2307/1924845,1979.

FAOSTAT: available at: https://www.fao.org/faostat/en/#data/GF, last access: 3 May 2022.

FAO FRA: FAO Global Forests Resource Assessment, available at fra-data.fao.org, last access: June 2022, 2022.

Friedlingstein, P., Jones, M. W., O'Sullivan, M., Andrew, R. M., Hauck, J., Peters, G. P., Peters, W., Pongratz, J., Sitch, S., Le Quéré, C., Bakker, D. C. E., Canadell, J. G., Ciais, P., Jackson, R. B., Anthoni, P., Barbero, L., Bastos, A., Bastrikov, V., Becker, M., Bopp, L., Buitenhuis, E., Chandra, N., Chevallier, F., Chini, L. P., Currie, K. I., Feely, R. A., Gehlen, M., Gilfillan, D., Gkritzalis, T., Goll, D. S., Gruber, N., Gutekunst, S., Harris, I., Haverd, V., Houghton, R. A., Hurtt, G., Ilyina, T., Jain, A. K., Joetzjer, E., Kaplan, J. O., Kato, E., Klein Goldewijk, K., Korsbakken, J. I., Landschützer, P., Lauvset, S. K., Lefèvre, N., Lenton, A., Lienert, S., Lombardozzi, D., Marland, G., McGuire, P. C., Melton, J. R., Metzl, N., Munro, D. R., Nabel, J. E. M. S., Nakaoka, S.-I., Neill, C., Omar, A. M., Ono, T., Peregon, A., Pierrot, D., Poulter, B., Rehder, G., Resplandy, L., Robertson, E., Rödenbeck, C., Séférian, R., Schwinger, J., Smith, N., Tans, P. P., Tian, H., Tilbrook, B., Tubiello, F. N., van der Werf, G. R., Wiltshire, A. J., and Zaehle, S.: Global Carbon Budget 2019, Earth Syst. Sci. Data, 11, 1783–1838, https://doi.org/10.5194/essd-11-1783-2019, 2019.

Friedlingstein, P., O'Sullivan, M., Jones, M. W., Andrew, R. M., Hauck, J., Olsen, A., Peters, G. P., Peters, W., Pongratz, J., Sitch, S., Le Quéré, C., Canadell, J. G., Ciais, P., Jackson, R. B., Alin, S., Aragão, L. E. O. C., Arneth, A., Arora, V., Bates, N. R., Becker, M., Benoit-Cattin, A., Bittig, H. C., Bopp, L., Bultan, S., Chandra, N., Chevallier, F., Chini, L. P., Evans, W., Florentie, L., Forster, P. M., Gasser, T., Gehlen, M., Gilfillan, D., Gkritzalis, T., Gregor, L., Gruber, N., Harris, I., Hartung, K., Haverd, V., Houghton, R. A., Ilyina, T., Jain, A. K., Joetzjer, E., Kadono, K., Kato, E., Kitidis, V., Korsbakken, J. I., Landschützer, P., Lefèvre, N., Lenton, A., Lienert, S., Liu, Z., Lombardozzi, D., Marland, G., Metzl, N., Munro, D. R., Nabel, J. E. M. S., Nakaoka, S.-I., Niwa, Y., O'Brien, K., Ono, T., Palmer, P. I., Pierrot, D., Poulter, B., Resplandy, L., Robertson, E., Rödenbeck, C., Schwinger, J., Séférian, R., Skjelvan, I., Smith, A. J. P., Sutton, A. J., Tanhua, T., Tans, P. P., Tian, H., Tilbrook, B., van der Werf, G., Vuichard, N., Walker, A. P., Wanninkhof, R., Watson, A. J., Willis, D., Wiltshire, A. J., Yuan, W., Yue, X., and Zaehle, S.: Global Carbon Budget 2020, Earth Syst. Sci. Data, 12, 3269–3340, https://doi.org/10.5194/essd-12-3269-2020, 2020.

Gilfillan, D., and Marland G.: CDIAC-FF: global and national CO_2 emissions from fossil fuel combustion and cement manufacture: 1751–2017, https://doi.org/10.5194/essd-13-1667-2021 , 2021.

Grassi, G., House, J., Kurz, W. A., Cescatti, A., Houghton, R. A., Peters, G. P., Sanz, M. J., Viñas, R. A., Alkama, R., Arneth, A., Bondeau, A., Dentener, F., Fader, M., Federici, S., Friedlingstein, P., Jain, A. K., Kato, E., Koven, C. D., Lee, D., Nabel, J. E. M. S., Nassikas, A. A., Perugini, L., Rossi, S., Sitch, S., Viovy, N., Wiltshire, A., and Zaehle, S.: Reconciling global-model estimates and country reporting of anthropogenic forest CO_2 sinks, Nat. Clim. Change, 8, 914–920, https://doi.org/10.1038/s41558-018-0283-x, 2018.

Grassi, G., Stehfest, E., Rogelj, J., van Vuuren, D., Cescatti, A., House, J., Nabuurs, G.-J., Rossi, S., Alkama, R., Viñas, R. A., Calvin, K., Ceccherini, G., Federici, S., Fujimori, S., Gusti, M., Hasegawa, T., Havlik, P., Humpenöder, F., Korosuo, A., Perugini, L., Tubiello, F. N., and Popp, A.: Critical adjustment of land mitigation pathways for assessing countries' climate progress, Nat. Clim. Change, 11, 425–434, https://doi.org/10.1038/s41558-021-01033-6, 2021.

Grassi, G., Conchedda, G., Federici, S., Abad Viñas, R., Korosuo, A., Melo, J., Rossi, S., Sandker, M., Somogyi, Z., and Tubiello, F. N.: Carbon fluxes from land 2000–2020: bringing clarity on countries' reporting, Biogeosciences and biodiversity, https://doi.org/10.5194/essd-2022-104, 2022.

Gütschow, J., Jeffery, M. L., Gieseke, R., Gebel, R., Stevens, D., Krapp, M., and Rocha, M.: The PRIMAP-hist national historical emissions time series, Earth Syst. Sci. Data, 8, 571–603, https://doi.org/10.5194/essd-8-571-2016, 2016.

Gütschow, J., Günther, A., Jeffery, M. L., and Gieseke, R.: The PRIMAP-hist national historical emissions time series (1850-2018) v2.2, https://doi.org/10.5281/zenodo.4479172, 2021.

Houghton, R. A., House, J. I., Pongratz, J., van der Werf, G. R., DeFries, R. S., Hansen, M. C., Le Quéré, C., and Ramankutty, N.: Carbon emissions from land use and land-cover change, Biogeosciences, 9, 5125–5142, https://doi.org/10.5194/bg-9-5125-2012, 2012.

IMF: International Monetary Fund: International Monetary Fund website, available at: https://www.imf.org/en/Publications/fandd/issues/Series/Back-to-Basics/gross-domestic-product-GDP, last access : February 2022.

IPCC: Good practice guidance for land use, land-use change and forestry /The Intergovernmental Panel on Climate Change. Edited by: Penman, J., Hayama, Kanagawa, 2006.

IPCC: Climate Change and Land: an IPCC special report on climate change, desertification, land degradation, sustainable land management, food security, and greenhouse gas fluxes in terrestrial ecosystems, [Shukla, P.R., Skea, J., CalvoBuendia,E., Masson-Delmotte, V., Pörtner, H.-O., Roberts, D. C., Zhai, P., Slade, R., Connors, S., van Diemen, R., Ferrat, M., Haughey, E., Luz, S., Neogi, S., Pathak, M., Petzold, J., Portugal Pereira, J., Vyas, P., Huntley, E., Kissick, K., Belkacemi, M., Malley,J. (eds.)]. In press, 2019.

IPCC: Revised 1996 IPCC Guidelines for National Greenhouse Inventories, IPCC/OECD/IEA, Paris, France, ISBN 92-64-15578- 3, 1997.

IPCC: 2006 IPCC guidelines for National Greenhouse Gas Inventories, IGES, ISBN 4-88788-032-4, 2006.

IPCC: 2019 Refinement to the 2006 IPCC Guidelines for National Greenhouse Gas Inventories, edited by: Buendia, E., Tanabe, K., Kranjc, A., Baasansuren, J., Fukuda, M., Ngarize, S., Osako, A., Pyrozhenko, Y., Shermanau, P., and Federici, S., Intergovernmental Panel on Climate Change (IPCC), Switzerland, ISBN 978-4-88788-232-4, 2019.

IPCC: Climate Change 2021: The Physical Science Basis. Contribution of Working Group I to the Sixth Assessment Report of the Intergovernmental Panel on Climate Change[Masson-Delmotte, V., P. Zhai, A. Pirani, S.L. Connors, C. Péan, S. Berger, N. Caud, Y. Chen, L. Goldfarb, M.I. Gomis, M. Huang, K. Leitzell, E. Lonnoy, J.B.R. Matthews, T.K. Maycock, T. Waterfield, O. Yelekçi, R. Yu, and B. Zhou (eds.)]. Cambridge University Press, Cambridge, United Kingdom and New York, NY, USA, In press, doi:10.1017/9781009157896, 2021.

Janssens-Maenhout, G., Pinty, B., Dowell, M., Zunker, H., Andersson, E., Balsamo, G., Bézy, J.-L., Brunhes, T., Bösch, H., Bojkov, B., Brunner, D., Buchwitz, M., Crisp, D., Ciais, P., Counet, P., Dee, D., Gon, H. D. van der, Dolman, H., Drinkwater, M. R., Dubovik, O., Engelen, R., Fehr, T., Fernandez, V., Heimann, M., Holmlund, K., Houweling, S., Husband, R., Juvyns, O., Kentarchos, A., Landgraf, J., Lang, R., Löscher, A., Marshall, J., Meijer, Y., Nakajima, M., Palmer, P. I., Peylin, P., Rayner, P., Scholze, M., Sierk, B., Tamminen, J., and Veefkind, P.: Toward an Operational Anthropogenic CO2 Emissions Monitoring and Verification Support Capacity, Bull. Am. Meteorol. Soc., 101, E1439–E1451, https://doi.org/10.1175/BAMS-D-19-0017.1, 2020.

1287
1288 van der Laan-Luijkx, I. T., van der Velde, I. R., van der Veen, E., Tsuruta, A., Stanislawska, K.,
1289 Babenhauserheide, A., Zhang, H. F., Liu, Y., He, W., Chen, H., Masarie, K. A., Krol, M. C., and Peters, W.:
1290 The CarbonTracker Data Assimilation Shell (CTDAS) v1.0: implementation and global carbon balance 2001–
1291 2015, Geosci. Model Dev., 10, 2785–2800, https://doi.org/10.5194/gmd-10-2785-2017, 2017.
1292
1293 Liousse, C., Assamoi, E., Criqui, P., Granier, C., and Rosset, R.: Explosive growth in African combustion
1294 emissions from 2005 to 2030, Environ. Res. Lett., 9, 035003, https://doi.org/10.1088/1748-9326/9/3/035003,
1295 2014.
1296
1297 Mostefaoui, M., Ciais, P., McGrath, M. J., Peylin, P., Prabir, P. K., Saunois, M., Chevallier, F., Sitch, S.,
1298 Rodenbeck, C., Luijkx, I., and Thompson, R.: Datasets for greenhouse gasses emissions and removals from
1299 inventories and global models over Africa v0.1, Zenodo [data set], https://doi.org/10.5281/zenodo.7347077,
1300 2022.
1301
1302 Monks, S. A., Arnold, S. R., Hollaway, M. J., Pope, R. J., Wilson, C., Feng, W., Emmerson, K. M., Kerridge,
1303 B. J., Latter, B. L., Miles, G. M., Siddans, R., and Chipperfield, M. P.: The TOMCAT global chemical transport
1304 model v1.6: description of chemical mechanism and model evaluation, Geosci. Model Dev., 10, 3025–3057,
1305 https://doi.org/10.5194/gmd-10-3025-2017, 2017.
1306
1307 Nickless, A., Scholes, R. J., Vermeulen, A., Beck, J., López-Ballesteros, A., Ardö, J., Karstens, U., Rigby, M.,
1308 Kasurinen, V., Pantazatou, K., Jorch, V., and Kutsch, W.: Greenhouse gas observation network design for
1309 Africa, Tellus B Chem. Phys. Meteorol., 72, 1–30, https://doi.org/10.1080/16000889.2020.1824486, 2020.
1310
1311 Patra, P. K., Takigawa, M., Watanabe, S., Chandra, N., Ishijima, K., and Yamashita, Y.: Improved Chemical
1312 Tracer Simulation by MIROC4.0-based Atmospheric Chemistry-Transport Model (MIROC4-ACTM), Sola,
1313 14, 91–96, https://doi.org/10.2151/sola.2018-016, 2018.
1314
1315 Perugini, L., Pellis, G., Grassi, G., Ciais, P., Dolman, H., House, J. I., Peters, G. P., Smith, P., Günther, D., and
1316 Peylin, P.: Emerging reporting and verification needs under the Paris Agreement: How can the research
1317 community effectively contribute?, Environ. Sci. Policy, 122, 116–126,
1318 https://doi.org/10.1016/j.envsci.2021.04.012, 2021.
1319
1320 Petrescu, A. M. R., Qiu, C., Ciais, P., Thompson, R. L., Peylin, P., McGrath, M. J., Solazzo, E., Janssens-
1321 Maenhout, G., Tubiello, F. N., Bergamaschi, P., Brunner, D., Peters, G. P., Höglund-Isaksson, L., Regnier, P.,
1322 Lauerwald, R., Bastviken, D., Tsuruta, A., Winiwarter, W., Patra, P. K., Kuhnert, M., Oreggioni, G. D., Crippa,
1323 M., Saunois, M., Perugini, L., Markkanen, T., Aalto, T., Groot Zwaaftink, C. D., Tian, H., Yao, Y., Wilson, C.,
1324 Conchedda, G., Günther, D., Leip, A., Smith, P., Haussaire, J.-M., Leppänen, A., Manning, A. J., McNorton,
1325 J., Brockmann, P., and Dolman, A. J.: The consolidated European synthesis of CH4 and N2O emissions for the
1326 European Union and United Kingdom: 1990–2017, Earth Syst. Sci. Data, 13, 2307–2362,
1327 https://doi.org/10.5194/essd-13-2307-2021, 2021.
1328
1329 Pongratz, J., Reick, C. H., Houghton, R. A., & House, J. I.: Terminology as a key uncertainty in net land use
1330 and land cover change carbon flux estimates. Earth System Dynamics, 5(1), 177-195.
1331 https://doi.org/10.5194/esd-5-177-2014, 2014.
1332
1333 PRIMAP-hist: PRIMAP-hist dataset, available at: https://www.pik-potsdam.de/paris-reality-check/primap-hist
1334 (last access: April 2022), 2021.
1335

1336 Rödenbeck, C.: Estimating CO2 sources and sinks from atmospheric mixing ratio measurements using a global
1337 inversion of atmospheric transport, undefined, 2005.
1338
1339 Rodgers, C. D.: Inverse Methods For Atmospheric Sounding: Theory And Practice, World Scientific, 256 pp.,
1340 2000.
1341
1342 Saunois, M., Stavert, A. R., Poulter, B., Bousquet, P., Canadell, J. G., Jackson, R. B., Raymond, P. A.,
1343 Dlugokencky, E. J., Houweling, S., Patra, P. K., Ciais, P., Arora, V. K., Bastviken, D., Bergamaschi, P., Blake,
1344 D. R., Brailsford, G., Bruhwiler, L., Carlson, K. M., Carrol, M., Castaldi, S., Chandra, N., Crevoisier, C., Crill,
1345 P. M., Covey, K., Curry, C. L., Etiope, G., Frankenberg, C., Gedney, N., Hegglin, M. I., Höglund-Isaksson, L.,
1346 Hugelius, G., Ishizawa, M., Ito, A., Janssens-Maenhout, G., Jensen, K. M., Joos, F., Kleinen, T., Krummel, P.
1347 B., Langenfelds, R. L., Laruelle, G. G., Liu, L., Machida, T., Maksyutov, S., McDonald, K. C., McNorton, J.,
1348 Miller, P. A., Melton, J. R., Morino, I., Müller, J., Murguia-Flores, F., Naik, V., Niwa, Y., Noce, S., O'Doherty,
1349 S., Parker, R. J., Peng, C., Peng, S., Peters, G. P., Prigent, C., Prinn, R., Ramonet, M., Regnier, P., Riley, W.
1350 J., Rosentreter, J. A., Segers, A., Simpson, I. J., Shi, H., Smith, S. J., Steele, L. P., Thornton, B. F., Tian, H.,
1351 Tohjima, Y., Tubiello, F. N., Tsuruta, A., Viovy, N., Voulgarakis, A., Weber, T. S., van Weele, M., van der
1352 Werf, G. R., Weiss, R. F., Worthy, D., Wunch, D., Yin, Y., Yoshida, Y., Zhang, W., Zhang, Z., Zhao, Y.,
1353 Zheng, B., Zhu, Q., Zhu, Q., and Zhuang, Q.: The Global Methane Budget 2000–2017, Earth Syst. Sci. Data,
1354 12, 1561–1623, https://doi.org/10.5194/essd-12-1561-2020, 2020.
1355
1356 Schulz, E., Speekenbrink, M., Krause, A.: A tutorial on Gaussian process regression: Modelling, exploring,
1357 and exploiting functions, Journal of Mathematical Psychology, https://doi.org/10.1016/j.jmp.2018.03.001,
1358 2018.
1359
1360 Sitch, S., Huntingford, C., Gedney, N., Levy, P. E., Lomas, M., Piao, S. L., Betts, R., Ciais, P., Cox, P.,
1361 Friedlingstein, P., Jones, C. D., Prentice, I. C., and Woodward, F. I.: Evaluation of the terrestrial carbon cycle,
1362 future plant geography and climate-carbon cycle feedbacks using five Dynamic Global Vegetation Models
1363 (DGVMs), Glob. Change Biol., 14, 2015–2039, https://doi.org/10.1111/j.1365-2486.2008.01626.x, 2008.
1364
1365 Thompson, R. L., Chevallier, F., Crotwell, A. M., Dutton, G., Langenfelds, R. L., Prinn, R. G., Weiss, R. F.,
1366 Tohjima, Y., Nakazawa, T., Krummel, P. B., Steele, L. P., Fraser, P., O'Doherty, S., Ishijima, K., and Aoki,
1367 S.: Nitrous oxide emissions 1999 to 2009 from a global atmospheric inversion, Atmospheric Chem. Phys., 14,
1368 1801–1817, https://doi.org/10.5194/acp-14-1801-2014, 2014.
1369
1370 Tian, H., Xu, R., Canadell, J. G., Thompson, R. L., Winiwarter, W., Suntharalingam, P., Davidson, E. A., Ciais,
1371 P., Jackson, R. B., Janssens-Maenhout, G., Prather, M. J., Regnier, P., Pan, N., Pan, S., Peters, G. P., Shi, H.,
1372 Tubiello, F. N., Zaehle, S., Zhou, F., Arneth, A., Battaglia, G., Berthet, S., Bopp, L., Bouwman, A. F.,
1373 Buitenhuis, E. T., Chang, J., Chipperfield, M. P., Dangal, S. R. S., Dlugokencky, E., Elkins, J. W., Eyre, B. D.,
1374 Fu, B., Hall, B., Ito, A., Joos, F., Krummel, P. B., Landolfi, A., Laruelle, G. G., Lauerwald, R., Li, W., Lienert,
1375 S., Maavara, T., MacLeod, M., Millet, D. B., Olin, S., Patra, P. K., Prinn, R. G., Raymond, P. A., Ruiz, D. J.,
1376 van der Werf, G. R., Vuichard, N., Wang, J., Weiss, R. F., Wells, K. C., Wilson, C., Yang, J., and Yao, Y.: A
1377 comprehensive quantification of global nitrous oxide sources and sinks, Nature, 586, 248–256,
1378 https://doi.org/10.1038/s41586-020-2780-0, 2020.
1379
1380 Tongwane, M. I. and Moeletsi, M. E.: A review of greenhouse gas emissions from the agriculture sector in
1381 Africa, Agric. Syst., 166, 124–134, https://doi.org/10.1016/j.agsy.2018.08.011, 2018.
1382 UNFCCC: UNFCCC: National Inventory Submissions, available at: https://unfccc.int/ (last access : March
1383 2021), 2021.
1384

1385 UNFCCC REDD+: REDD+ National Reports, available at: https://redd.unfccc.int/submissions.html?topic=6
1386 (last access: July 2022), 2022.
1387 United Nations Department of Economic and Social Affairs, Population Division: World Population Prospects
1388 2019: Summary of Results, 2019.
1389
1390 Valentini, R., Arneth, A., Bombelli, A., Castaldi, S., Cazzolla Gatti, R., Chevallier, F., Ciais, P., Grieco, E.,
1391 Hartmann, J., Henry, M., Houghton, R. A., Jung, M., Kutsch, W. L., Malhi, Y., Mayorga, E., Merbold, L.,
1392 Murray-Tortarolo, G., Papale, D., Peylin, P., Poulter, B., Raymond, P. A., Santini, M., Sitch, S., Vaglio Laurin,
1393 G., van der Werf, G. R., Williams, C. A., and Scholes, R. J.: A full greenhouse gases budget of Africa: synthesis,
1394 uncertainties, and vulnerabilities, Biogeosciences, 11, 381–407, https://doi.org/10.5194/bg-11-381-2014, 2014.
1395
1396 van der Werf, G. R., Randerson, J. T., Giglio, L., van Leeuwen, T. T., Chen, Y., Rogers, B. M., Mu, M., van
1397 Marle, M. J. E., Morton, D. C., Collatz, G. J., Yokelson, R. J., and Kasibhatla, P. S.: Global fire emissions
1398 estimates during 1997–2016, Earth Syst. Sci. Data, 9, 697–720, https://doi.org/10.5194/essd-9-697-2017, 2017.
1399
1400 Wilson, C., Chipperfield, M. P., Gloor, M., and Chevallier, F.: Development of a variational flux inversion
1401 system (INVICAT v1.0) using the TOMCAT chemical transport model, Geosci. Model Dev., 7, 2485–2500,
1402 https://doi.org/10.5194/gmd-7-2485-2014, 2014.
1403
1404 World   Bank: GDP   exchange   rate   estimates,   available   at
1405 https://data.worldbank.org/indicator/NY.GDP.MKTP.CD last accessed, 2019.
1406
1407 World Bank: World Bank economic data, available at: https://www.worldbank.org/ (last access: May 2022),
1408 2022.
1409
1410 Zhu, Y., Merbold, L., Pelster, D., Diaz-Pines, E., Wanyama, G. N., and Butterbach-Bahl, K.: Effect of Dung
1411 Quantity and Quality on Greenhouse Gas Fluxes From Tropical Pastures in Kenya, Glob. Biogeochem. Cycles,
1412 32, 1589–1604, https://doi.org/10.1029/2018GB005949, 2018.
1413
1414 van der Zwaan, B., Kober, T., Longa, F. D., van der Laan, A., and Jan Kramer, G.: An integrated assessment
1415 of pathways for low-carbon development in Africa, Energy Policy, 117, 387–395,
1416 https://doi.org/10.1016/j.enpol.2018.03.017, 2018.
1417